TWO PROPERTIES OF THE RIEMANN ZETA FUNCTION ZEROS

HUBERT SCHAETZEL

ABSTRACT. The purpose of this article is to give proofs, in fact closely related one to each other, of the Riemann hypothesis, hypothesis which states that all non-trivial zeros of the Zeta function are on the critical line. Ahead of that, we will establish that there are no double zeros of the said function, result which is also a novel contribution.

Contents

1. The tools	1
2. The absence of double zeros of the Zeta function	4
3. The half-wave phase shift proof	8
4. The analytic proof	15
5. The complex plane graphical context	21
5.1. The standard context	21
5.2. Understanding the standard context	26
5.3. The simplified context	35
5.4. A mix graphic-analytic proof	36
6. An alternative graphical context and proof	44
7. The partial cancellations' network	49
7.1. Covering the left half critical band	49
7.2. Axis intersections	51
Literature and sources	58

1. The tools

The Riemann Zeta function is defined over the complex half-plane Re(s) > 1 by

$$\zeta(s) = \sum_{n=1}^{\infty} \frac{1}{n^s}$$

where $s = \sigma + i.t$ is the standard notation of the complex variable s. This function has an analytic continuation over the whole complex plane except at

Date: October 19, 2025.

²⁰²⁰ Mathematics Subject Classification. 11M26, 30C35.

Key words and phrases. Riemann hypothesis, conformal map.

its unique pole s=1+0.i. The resulting function is therefore a meromorphic function according to the following definitions.

Definition 1. A function f is holomorphic on an open set D in the complex plane if, for any $z_0 \in D$, one can write

$$f(z) = \sum_{n=0}^{\infty} a_n (z - z_0)^n$$

in which the coefficients a_n are complex numbers and the series is convergent to f(z) for z in a neighbourhood of z_0 .

Alternatively, a complex analytic function is an infinitely differentiable function such that the Taylor series at any point z_0 in its domain converges to f(z) for z in a neighbourhood of z_0 pointwise. (See reference [14]).

Definition 2. A meromorphic function on an open subset D of the complex plane is holomorphic on all of D except for a set of isolated points, which are the poles of the function. (See reference [14]).

These reminders being made, the following theorems will also be useful later on.

Theorem 1. Isolated zeros principle.

The zeros of a non-constant analytic function are isolated.

Theorem 2. If U is an open subset of the complex plane \mathbb{C} , then a function $f:U\to\mathbb{C}$ is conformal if and only if it is holomorphic and its derivative is everywhere non-zero on U. The Riemann mapping theorem states that any non-empty open simply connected proper subset of \mathbb{C} admits a bijective conformal map to the open unit disk in \mathbb{C} .

Proof. See reference [13]. Note that the theorem applies to a function f of one and only one variable s.

Theorem 3. According to the Abel summation formula, for Re(s) > 0, the Zeta function can be expressed as

$$\zeta(s) = \frac{s}{s-1} - s \int_1^\infty \frac{\{u\}}{u^{1+s}} du$$

where $\{u\}$ is the mantissa of u.

Proof. See reference [11].

Theorem 4. Besides, the Dirichlet Eta function is another analytical continuation of the Zeta function, valid this time, for 0 < Re(s) < 1, and writes down as

$$\eta(s) = \frac{1}{1 - 2^{1 - s}} \sum_{n=1}^{\infty} \frac{(-1)^{n-1}}{n^s}$$

Proof. See reference [11].

The Riemann's hypothesis, formulated in 1859 [1] [10], is that the nontrivial zeros of the function are such that $Re(s) = \frac{1}{2}$, the zeros quoted as trivial being $s=-2n, n\in N^*$. This can be illustrated by the traditional figure 1.

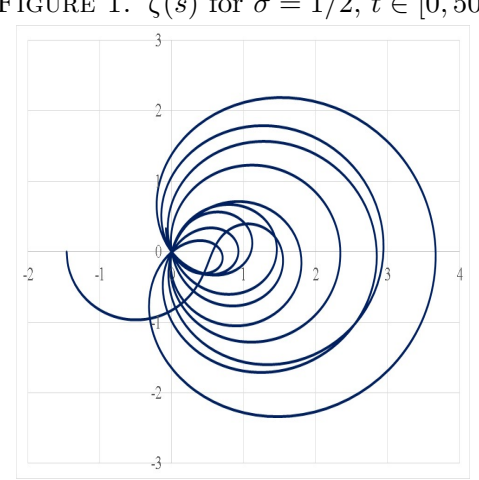


FIGURE 1. $\zeta(s)$ for $\sigma = 1/2, t \in [0, 50]$

A well-established result is that all the non-trivial zeros are located within the critical band 0 < Re(s) < 1. In search of zeros, one can reduce the review to the domain $0 < \sigma \le 1/2$ (or $1/2 \le \sigma < 1$) thanks to the following fact:

Theorem 5. Within the critical band, the non-trivial ζ -function zeros are symmetrical to the axis s = 1/2.

Proof. It is an immediate result of the functional equation (see references [2] and [11])

$$\zeta(s) = 2^s \pi^{s-1} \sin \frac{\pi s}{2} \Gamma(1-s) \zeta(1-s),$$

in which the expression $2^s \pi^{s-1} \sin \frac{\pi s}{2} \Gamma(1-s)$ never cancels if $0 < \sigma < 1$. \square

Lemma 1. The n^{th} derivative of the Zeta function is

$$\zeta^{(n)}(s) = if(n = 0, 1, 0) + (-1)^n \left(\frac{n!}{(s-1)^{n+1}} + n \int_1^\infty \frac{\ln^{n-1}(u)\{u\}}{u^{1+s}} du - s \int_1^\infty \frac{\ln^n(u)\{u\}}{u^{1+s}} du\right).$$

Proof. The equation is true for n = 0. The proof is deduced by induction on the parameter n. One can also use the n^{th} derivative of $\zeta(s)-1$ to write $\zeta^{(n)}(s)$ – if $(n=0,1,0)=(\zeta(s)-1)^{(n)}$ in order to avoid the n=0 peculiar case within the former formula.

The Pari gp on-line application is chosen here whenever we wish to provide some numerical data and the resulting illustrations are given after injecting the data on an Excel spreadsheet.

Given some coordinate $s = \sigma + i.t$ value, we will call, here and there, σ the abscissa and t the ordinate.

2. The absence of double zeros of the Zeta function

Theorem 6. The Riemann Zeta function and its first derivative never cancel simultaneously, that is there is no solution s such that $\zeta(s) = \zeta'(s) = 0$.

Proof. Let us suppose Re(s) > 0. Recalling theorem 3, let us take the derivatives on each side of the corresponding expression. We get using the product rule for derivatives

$$\begin{array}{lcl} \zeta'(s) & = & -\frac{s}{(s-1)^2} + (\frac{1}{s-1} - \int_1^\infty \frac{\{u\}}{u^{1+s}du}) + s \int_1^\infty \frac{(\ln(u))\{u\}}{u^{1+s}} du \\ & = & -\frac{s}{(s-1)^2} + \frac{\zeta(s)}{s} + s \int_1^\infty \frac{(\ln(u))\{u\}}{u^{1+s}} du \end{array}$$

Then (again using 3)

$$\int_{1}^{\infty} \frac{\{u\}}{u^{1+s}} du = \frac{1}{s-1} - \frac{\zeta(s)}{s}$$

and (from the expression de $\zeta'(s)$)

$$\int_{1}^{\infty} \frac{(\ln(u))\{u\}}{u^{1+s}} du = \frac{1}{(s-1)^2} - \frac{\zeta(s)}{s^2} + \frac{\zeta'(s)}{s}.$$

Thus

$$\frac{\int_{1}^{\infty} \frac{(\ln(u))\{u\}}{u^{1+s}} du}{(\int_{1}^{\infty} \frac{\{u\}}{u^{1+s}} du)^{2}} = \frac{\frac{1}{(s-1)^{2}} - \frac{\zeta(s)}{s^{2}} + \frac{\zeta'(s)}{s}}{(\frac{1}{s-1} - \frac{\zeta(s)}{s})^{2}} \\
= \frac{\frac{1}{(s-1)^{2}} - 2\frac{\zeta(s)}{s(s-1)} + (\frac{\zeta(s)}{s})^{2} - \frac{\zeta(s)}{s^{2}} + \frac{\zeta'(s)}{s} + 2\frac{\zeta(s)}{s(s-1)} - (\frac{\zeta(s)}{s})^{2}}{\frac{1}{(s-1)^{2}} - 2\frac{\zeta(s)}{s(s-1)} + (\frac{\zeta(s)}{s})^{2}} \\
= 1 + \frac{-\frac{\zeta(s)}{s^{2}} + \frac{\zeta'(s)}{s} + 2\frac{\zeta(s)}{s(s-1)} - (\frac{\zeta(s)}{s})^{2}}{(\frac{1}{s-1} - \frac{\zeta(s)}{s})^{2}} \\
= 1 + \frac{\frac{1}{s}(\zeta'(s) + \zeta(s)(\frac{s+1}{s(s-1)} - \frac{\zeta(s)}{s}))}{(\frac{1}{s-1} - \frac{\zeta(s)}{s})^{2}}$$

Let us have s_0 a double root (at least) of the Zeta function, that is $\zeta(s_0) = \zeta'(s_0) = 0$.

Then

$$\int_{1}^{\infty} \frac{\{u\}}{u^{1+s_0}} du = \frac{1}{s_0 - 1}$$

and

$$\int_{1}^{\infty} \frac{(\ln(u))\{u\}}{u^{1+s_0}} du = \frac{1}{(s_0 - 1)^2}$$

and therefore

$$\frac{\int_{1}^{\infty} \frac{(\ln(u))\{u\}}{u^{1+s_0}} du}{(\int_{1}^{\infty} \frac{\{u\}}{u^{1+s_0}} du)^2} = 1$$

The Riemann Zeta function is continuous. Therefore, when $s \to s_0$, we get

$$\frac{\frac{1}{s}(\zeta'(s) + \zeta(s)(\frac{s+1}{s(s-1)} - \frac{\zeta(s)}{s}))}{(\frac{1}{s-1} - \frac{\zeta(s)}{s})^2} \to 0$$

while the following expressions tend towards fixed non-null values

$$\frac{1}{s} \to \frac{1}{s_0} \text{ and } (\frac{1}{s-1} - \frac{\zeta(s)}{s})^2 \to (\frac{1}{s_0 - 1} - \frac{\zeta(s_0)}{s_0})^2 \to \frac{1}{(s_0 - 1)^2}$$

Therefore, as $\zeta(s) \to \zeta(s_0) = 0$, we get

$$\zeta'(s) + \zeta(s)\left(\frac{s+1}{s(s-1)} - \frac{\zeta(s)}{s}\right) \to \zeta'(s) + \frac{s+1}{s(s-1)}\zeta(s) \to 0$$

Thus, the zeros being isolated, and therefore $\zeta(s) \neq 0$, it follows

$$\frac{\zeta'(s)}{\zeta(s)} \to -\frac{s+1}{s(s-1)}$$

Let us choose some complex coordinate s, not a zero but close to a non-trivial zero s_0 of ζ , thus $s=s_0+\Delta s_0$, with n the multiplicity of the zero s_0 . With this choice, the complex value s has an inverse. There is no zero near the pole of the studied function and therefore we can also make the choice of s such that 1/(s-1) and $1/(s_0-1)$ have always finite values in our arguments. From definitions 2 and 1, the terms of higher degrees being negligible in the Taylor series, we deduce

$$\zeta(s) \to \alpha(s-s_0)^n \text{ as } s \to s_0$$

where α is some finite non-zero value. The number n being the multiplicity of the zero s_0 , we are interested in the cases $n \ge 2$. Let us start by evaluating the first derivative near that zero

$$\zeta'(s) \to n\alpha(s-s_0)^{n-1}$$
 as $s \to s_0$

Therefore

$$\frac{\zeta'(s)}{\zeta(s)} \to \frac{n}{s - s_0}$$
 as $s \to s_0$

Thus we have necessarily

$$\frac{n}{s-s_0} \to -\frac{s+1}{s(s-1)}$$

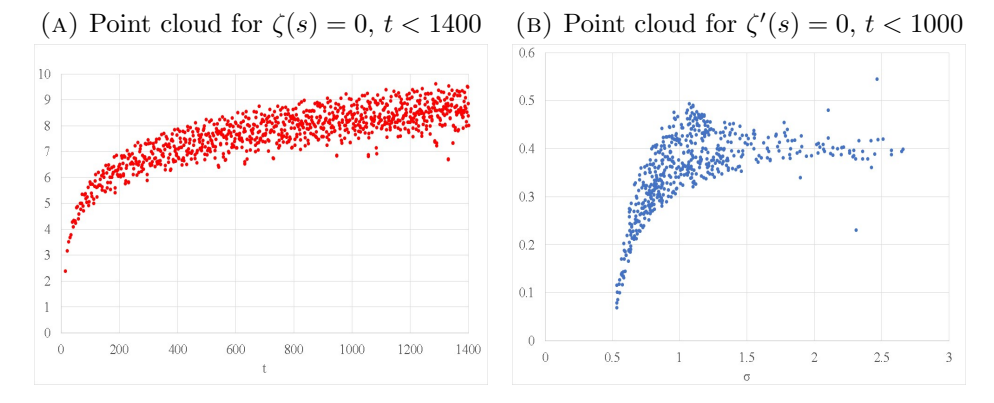
As s tends towards s_0 , the first term is diverging so that $s \to 0$ or $s \to 1$ (if $s \to +\infty$, the second term is tending towards 0 and cannot be a solution). But there are definitively no zeros of the Riemann Zeta function near the coordinates s = 0 or s = 1, therefore the hypothesis $\zeta(s_0) = \zeta'(s_0) = 0$ is impossible. The result being true within the critical band, it is true in the whole complex plane.

Note. One may find interesting to evaluate in some way the "distance" that exists really to the simultaneous events $\zeta(s)=0$ and $\zeta'(s)=0$. That can be done, for example, by evaluating the ratio $\int_1^\infty \frac{(ln(u))\{u\}}{u^{1+s}} du/(\int_1^\infty \frac{\{u\}}{u^{1+s}} du)^2$ and comparing it to 1. The strategy could be to research the closest value to 1 within the critical band as t is taking increasing values. This is however somewhat cumbersome to implement. We choose here to get the point clouds of the ratio when only one of the events occurs. It won't give the optimum

data but the approach still gives some notable information. The figures 2A and 2B represents the point clouds obtained. These figures provide the Napierian logarithm and therefore the two events' coincidence would to achieved for Ln(1)=0, hence at the ordinate 0. Figure 2A shows that the more likely solutions, if they existed, would be near t=0, an expected consequence of the former proof. As there is no expected case where $\zeta'(s)=0$ for $\sigma<1/2$ (see reference [4]), there can be no tendency towards $\sigma=0$ in the second point cloud, the way it is calculate. In figure 2B, we see instead a tendency towards the average value of the expected s=0 or s=1 (thus $\sigma=(0+1)/2$). We see also that the upper side of the point cloud culminates mainly around $\sigma=1$ and the point cloud get its broadest size around that abscissa. To finish with, let us note also that the four points that are "escaping" the point cloud are part of the seven first solutions of $\zeta'(s)=0$, where 0< t<70, an interval where the $\frac{s}{s-1}$ contribution in the Abel summation of $\zeta(s)$ is still of some highly differentiating importance.

Figure 2. Point clouds of
$$f=Ln(\frac{\int_1^\infty \frac{(\ln(u))\{u\}}{u^{1+s}}du}{(\int_1^\infty \frac{\{u\}}{u^{1+s}}du)^2})$$

$$\zeta(s)=\zeta'(s)=0 \text{ if } f=0.$$



Let us have also a glance at a sample of trajectories $\zeta(s)$, at constant $t=t_0$, where $\zeta'(\sigma_0+i.t_0)=0$ occurs for values of σ_0 close to 1/2. Let us focus on the evolution of the curves while σ increases from some value lower than 1/2 (here 1/4) up to σ quite larger than 1/2 (here 5). The reader will then notice immediately the reverse direction at the abscissas σ_0 cancelling the derivative of the function as if there was some kind of repulsive force from 0 operating as the curves head closer to 0.

This results in the trajectories pointing towards 0 at the said events $\zeta'(s_0) = 0$. This pointing phenomena won't of course necessarily persist when σ is significantly larger then 0.5 (let say for example 0.6) but gets quite obvious as the value of σ gets closer to 1/2 (let say for example < 0.55). Hence, there is naturally a great temptation to correlate the mentioned repulsion to the interdiction of any double zero.

Figure 3A shows a sample of examples. For the chosen t_0 values, we have $\zeta'(s_0) = 0$ for some $\sigma_0 > 1/2$, indicated in the figure's header, and we chose here the sample with the smallest σ_0 values occurring through out the interval $0 < t_0 < 1000$. Thus, on the basis of this graphic, to envisage $\sigma_0 < 1/2$, while $\zeta'(s_0) = 0$, seems already altogether absurd.

Now we may raise the question if there is some way to prolong the trajectories of the curves towards the seemingly 0 aim. We know that analytic functions generate conformal maps. Thus angles in the domain are conserved in the image except at domain coordinates where the derivative cancels in which cases the angles double. Prolonging trajectories straight ahead means introducing π angles. Requiring it, at some derivative cancellation's coordinate, is therefore, in the domain, an angle equal to $\frac{\pi}{2}$ which, in the complex plane, is equivalent to a multiplication by the complex number i. This means, instead of s, we ought to use i.s, a move that exchanges the role of σ and t in our specific context: In figure 3A, σ was the variable and t was fixed. Choosing to prolong trajectories in the way we just described means now to have t to be the variable and σ to be fixed. In figure 3B, we implement the trajectories extension in dotted lines. The doubling of angles, in conformal mappings' context, exists only at the derivative cancellation coordinates while the conservation of angles takes effect immediately after such events. It produces a progressive enlargement of the angle between the inwards and the outwards pieces of dotted trajectories, phenomena which again may be interpreted as some kind of repulsion as the coordinate 0 gets closer. The "middle" trajectory of that dotted prolongation however would again approximatively head towards 0 the closer σ_0 to 0.

```
FIGURE 3. Trajectories of \zeta(s), \sigma \in [1/4, 5].

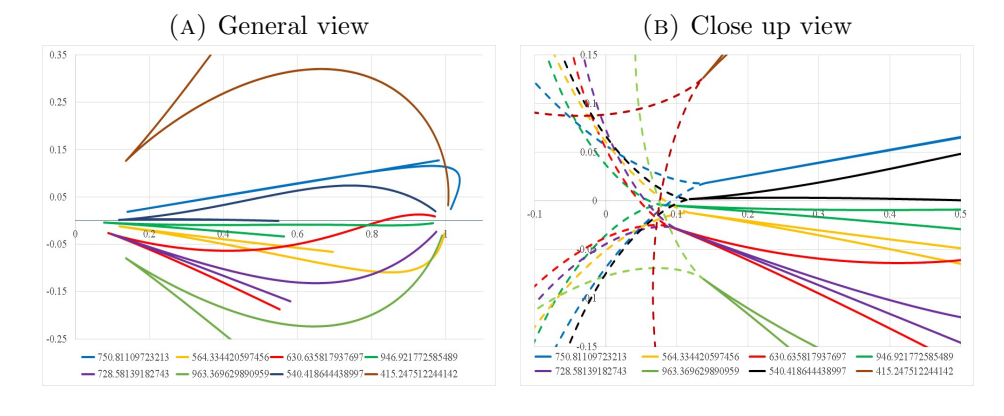
\zeta'(s_0) = 0 at the coordinates (\sigma_0, t_0) \approx

(0.529499, 750.81110), (0.531397, 946.92177),

(0.532358, 630.63582), (0.534289, 564.33442),

(0.537986, 728.58139), (0.548197, 963.36963),

(0.550028, 540.41864), (0.551299, 415.24751).
```



To be precise, what we have shown here is that there is an effective barrier to the simultaneous events $\zeta(s)$ and $\zeta'(s)$ tending together towards 0, but the involvement of the limit $\sigma = \frac{1}{2}$ is only derived here from a sample of numerical observations. Therefore, let us add some arguments although those are not rigorous. If $\zeta(s) \to 0$, using the functional equation, we get $\zeta(1-s) \to 0$. If we add the constraint $\zeta'(s) \to 0$ and use the derivation of the functional equation, we get $\zeta'(s) = (2^s \pi^{s-1} \sin \frac{\pi s}{2} \Gamma(1-s))' \zeta(1-s) + 2^s \pi^{s-1} \sin \frac{\pi s}{2} \Gamma(1-s) \zeta'(1-s)$. Therefore $\zeta'(s) \to 2^s \pi^{s-1} \sin \frac{\pi s}{2} \Gamma(1-s) \zeta'(1-s)$, thus finally $\zeta'(1-s) \to 0$. It means that $\zeta(s)$ and its derivative tend towards $\zeta(1-s)$ and its derivative. If we take that for granted in the vicinity of s also, $\zeta(s)$ and $\zeta(1-s)$ would locally be approximatively the same. The image trajectories being more or less the same, we could then assume it in the domain also. This means $s \to 1-s$ or $s \to \frac{1}{2}$. Observe that the two cancellations' constraint leads to a much stronger conclusion then the one we initially hoped for, namely $\sigma \to \frac{1}{2}$, the discrepancy lying either in the impossibility to have $\zeta'(s) = 0$ on the left side of the critical line (therefore an impossible symmetry) or\and the trivial non-bijectivity between the domain s and the image $\zeta(s)$.

To finish this section, let us add a correlated lemma.

Lemma 2. The function $\varpi(s) = \frac{\zeta}{\zeta'}(s)$ has no double zeros.

Proof. The function is defined for $\zeta'(s) \neq 0$. Deriving, we get $\varpi'(s) = (\frac{\zeta(s)}{\zeta'(s)})' = \frac{(\zeta'(s))^2 - \zeta(s)\zeta''(s)}{(\zeta'(s))^2}$. This expression cancels if and only if $(\zeta'(s))^2 - \zeta(s)\zeta''(s)$. Supposing we already have $\varpi(s) = 0$, which implies $\zeta(s) = 0$, we get $(\zeta'(s))^2 = 0$ that is $\zeta'(s) = 0$. Therefore the function ϖ may have a double zero only if the function ζ has a double zero, which by now we know is impossible.

3. The half-wave phase shift proof

In the following development, we will see that focusing mainly on the cancelling property of the zeros of the Riemann Zeta function may be irrelevant and rather a trap to address the Riemann hypothesis. Only the symmetry of the zeros towards the critical line is necessary to meet an interesting result.

Let us investigate the real and imaginary parts of the Zeta function. Let us have $\chi(1/2, \Delta, t) = \zeta(1/2 - \Delta + i.t) - \zeta(1/2 + \Delta + i.t)$. We want to solve $\chi(1/2, \Delta, t) = 0$ where Δ is real valued again. Then $\chi(1/2, \Delta, t) = Re(\zeta(1/2 - \Delta + i.t)) - Re(\zeta(1/2 + \Delta + i.t)) + i.(Im(\zeta(1/2 - \Delta + i.t)) - Im(\zeta(1/2 + \Delta + i.t))) = 0$. Cancelling the expression means at least therefore

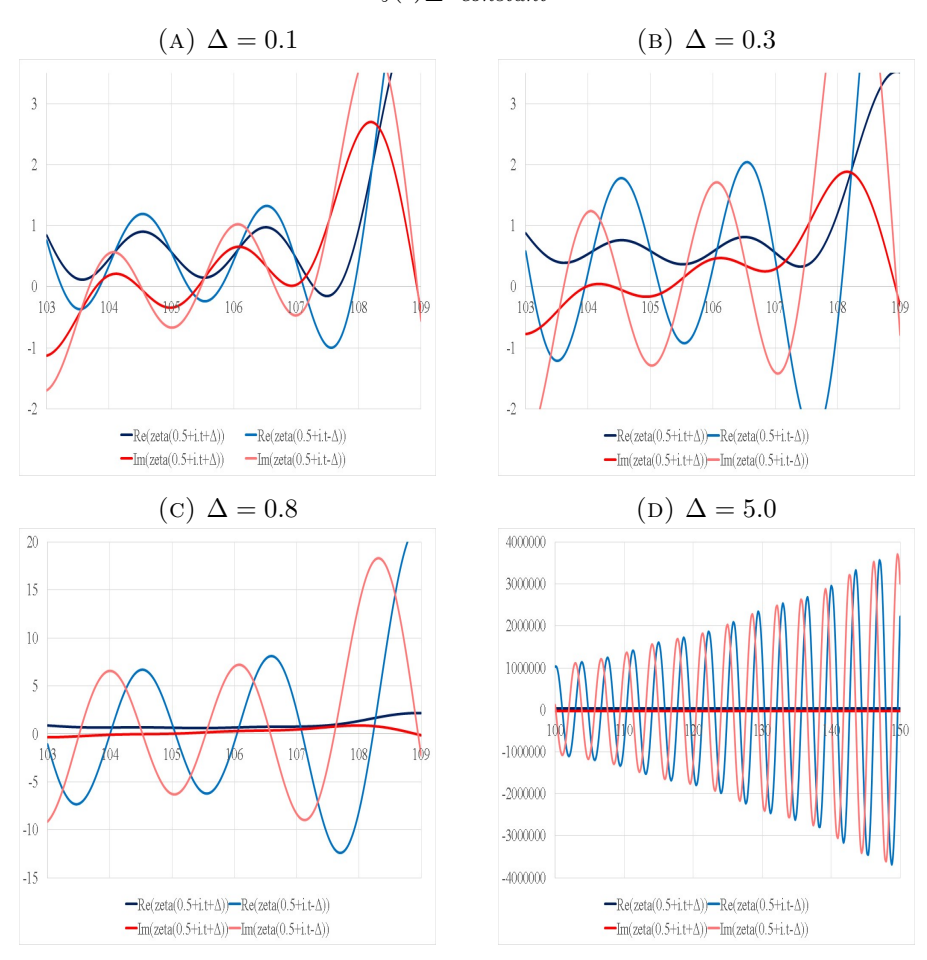
$$Re(\zeta(1/2 - \Delta + i.t)) = Re(\zeta(1/2 + \Delta + i.t))$$

$$Im(\zeta(1/2 - \Delta + i.t)) = Im(\zeta(1/2 + \Delta + i.t))$$

Here of course, we examine only the cases where $\Delta \neq 0$, the equalities being trivial otherwise. The figures 4A to 4C give a sample of the evolution

of each of the members of these equalities $Re(\zeta(1/2 - \Delta + i.t))$, $Re(\zeta(1/2 + \Delta + i.t))$, $Im(\zeta(1/2 - \Delta + i.t))$ and $Im(\zeta(1/2 + \Delta + i.t))$ over the interval $t \in [103, 109]$. In these figures, one has to focus on the intersection positions of similar color curves. One will observe, when $Re(\zeta(1/2 - \Delta + i.t)) = Re(\zeta(1/2 + \Delta + i.t))$ that, at the same position t, the difference $Im(\zeta(1/2 - \Delta + i.t)) - Im(\zeta(1/2 + \Delta + i.t))$ is heading towards some approximative maximum, therefore a non-null value. The same occurs when $Im(\zeta(1/2 - \Delta + i.t)) = Im(\zeta(1/2 + \Delta + i.t))$, with this time the difference $Re(\zeta(1/2 - \Delta + i.t)) - Re(\zeta(1/2 + \Delta + i.t))$ in "search of" some maximum.

FIGURE 4. Trajectories real and imaginary parts of $\zeta(t)_{\Delta=constant}.$



This is an immediate consequence of theorem 4. The Zeta function and the Dirichlet Eta function share the same zeroes within the critical band. The Zeta function is merely a slightly deformed version, by the $\frac{1}{1-2^{1-s}}$ factor, of the sum

$$\begin{array}{ll} \sum_{n=1}^{\infty} \frac{(-1)^{n-1}}{n^s} &= \sum_{n=1}^{\infty} \frac{(-1)^{n-1}}{n^{\sigma}} (\cos(\ln(n).t) - i.\sin(\ln(n).t)) \\ &= \sum_{n=1}^{\infty} \frac{(-1)^n}{n^{\sigma}} (\sin(\ln(n).t - \frac{\pi}{2}) + i.\sin(\ln(n).t)) \end{array}$$

Here the $\frac{\pi}{2}$ phase shift between the real and imaginary parts leads naturally to the alternating minima (that is a null value) and maxima of the differences between $Re(\zeta(1/2-\Delta+i.t))-Re(\zeta(1/2+\Delta+i.t))$ and $Im(\zeta(1/2-\Delta+i.t))-Im(\zeta(1/2+\Delta+i.t))$. Therefore, if three entities among $Re(\zeta(1/2-\Delta+i.t))$, $Re(\zeta(1/2+\Delta+i.t))$, $Im(\zeta(1/2-\Delta+i.t))$ and $Im(\zeta(1/2+\Delta+i.t))$ take nearly the same value, the fourth one will necessarily distance itself from that common value (hence confirming the Riemann hypothesis).

Note. The $\frac{\pi}{2}$ phase shift is an indisputable fact and therefore, there is no need for three close values to get a nearby maximal difference for the fourth item. The intersection of two blue tone curve will result in two red tone curve distancing and the same inverting the color tones. But one will likely head towards an absolute maximum difference situation rather than a vague middle tendency in the case of a "three common". Note however that three close value doesn't mean at all broader peaks or broader differences. It is not a matter of size but of existence.

Note. The crossings of $Re(\zeta(1/2-\Delta+i.t))$ with $Re(\zeta(1/2+\Delta+i.t))$, respectively $Im(\zeta(1/2-\Delta+i.t))$ with $Im(\zeta(1/2+\Delta+i.t))$, as Δ increases steadily, are heading locally to equal spaced intervals (on the t axis) as $Re(\zeta(1/2+\Delta+i.t))$, respectively $Im(\zeta(1/2+\Delta+i.t))$, become negligible in regard to $Re(\zeta(1/2-\Delta+i.t))$, respectively $Im(\zeta(1/2-\Delta+i.t))$, and the former $Re(\zeta(1/2+\Delta+i.t))$, respectively $Im(\zeta(1/2+\Delta+i.t))$, are meanwhile heading towards local almost sinusoidal curves. We call them local because of the simultaneous exponential growth of the amplitude with t. In fact, the whole underlining pattern in work in the figures 4C to 4A is merely a deformation, as the value of Δ is shrinking, of two local sinusoids (let us say one sine and the other a cosine and two lines, one at approximate ordinate 1 representing $Re(\zeta(1/2+\Delta+i.t))$ and the other at approximate ordinate 0 for $Im(\zeta(1/2+\Delta+i.t))$, as illustrated by the figure 4D for a larger interval of the parameter t. That deformation despite not being uniform keeps the alternating intersections of same tone color curves in the same order.

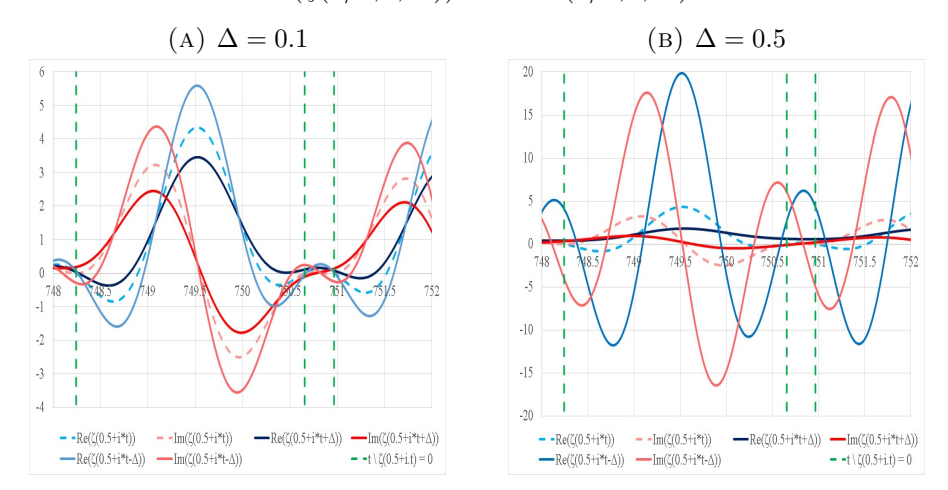
Note. We added the curves for $\Delta=0$ in the figures 5A and 5B to show that the intersections of likewise color curves don't match with the positions t of the zeros of the Zeta function.

Note. One may still object that the Zeta function is not $\sum_{n=1}^{\infty} \frac{(-1)^{n-1}}{n^s}$, but $\frac{1}{1-2^{1-s}} \sum_{n=1}^{\infty} \frac{(-1)^{n-1}}{n^s}$ and therefore that function must verify the half-wave shift we argued above. So let us do that verification. For that, we will write $\frac{1}{1-2^{1-s}} \sum_{n=1}^{\infty} \frac{(-1)^{n-1}}{n^s} = \sum_{n=1}^{\infty} \frac{(-1)^{n-1}n^{-s}}{1-2^{1-s}} = \sum_{n=1}^{\infty} \frac{(-1)^{n-1}n^{-\sigma-i.t}}{1-2^{1-\sigma-i.t}} = \sum_{n=1}^{\infty} \frac{(-1)^{n-1}}{n^{\sigma}} \frac{(\cos(t.\ln(n)) - i.\sin(t.\ln(n)))(1-2^{1-\sigma}(\cos(t.\ln(2)) - i.\sin(t.\ln(2))))}{(1-2^{1-\sigma}\cos(t.\ln(2)))^2 + (2^{1-\sigma}\sin(t.\ln(2)))^2}$

$$\begin{aligned} &\cos(t.\ln(n)) - 2^{1-\sigma}\cos(t.\ln(2)).\cos(t.\ln(n)) - 2^{1-\sigma}\sin(t.\ln(2)).\sin(t.\ln(n)) \\ &= \sum_{n=1}^{\infty} \frac{(-1)^{n-1}}{n^{\sigma}} \frac{+i.(-\sin(t.\ln(n)) + 2^{1-\sigma}\cos(t.\ln(2)).\sin(t.\ln(n)) - 2^{1-\sigma}\sin(t.\ln(2)).\cos(t.\ln(n))}{1 + 2^{2(1-\sigma)} - 2^{2-\sigma}\cos(t.\ln(2))} \\ &= \frac{1}{1 + 2^{2(1-\sigma)} - 2^{2-\sigma}\cos(t.\ln(2))} \sum_{n=1}^{\infty} \frac{(-1)^{n-1}}{n^{\sigma}} {\cos(t.\ln(n)) - 2^{1-\sigma}\cos(t.\ln(n/2)) - i.(\sin(t.\ln(n)) - 2^{1-\sigma}\sin(t.\ln(n/2))) \\ &= \frac{1}{1 + 2^{2(1-\sigma)} - 2^{2-\sigma}\cos(t.\ln(2))} \sum_{n=1}^{\infty} \frac{(-1)^{n-1}}{n^{\sigma}} {\cos(t.\ln(n)) - 2^{1-\sigma}\cos(t.\ln(n/2)) - i.(\cos(\frac{\pi}{2} + t.\ln(n)) - 2^{1-\sigma}\cos(\frac{\pi}{2} + t.\ln(n/2))) \end{aligned}$$

The fraction in front of the sum depends on t, but it acts only as a same scaling real variable on each corresponding real and imaginary term of the sum, therefore not affecting the half-wave phase shift between those two.

FIGURE 5. Trajectories real and imaginary parts of $Re(\zeta(1/2, t, \Delta))$ and $Im(1/2, t, \Delta)$.



Theorem 7. The Riemann hypothesis is true.

Proof. Having simultaneously $Re(\zeta(1/2-\Delta+i.t))=Re(\zeta(1/2+\Delta+i.t))=Im(\zeta(1/2-\Delta+i.t))=Im(\zeta(1/2+\Delta+i.t))=Im(\zeta(1/2+\Delta+i.t))$ is impossible and therefore even more so the whole line of equalities equal to 0. Hence the above theorem remembering theorem 5.

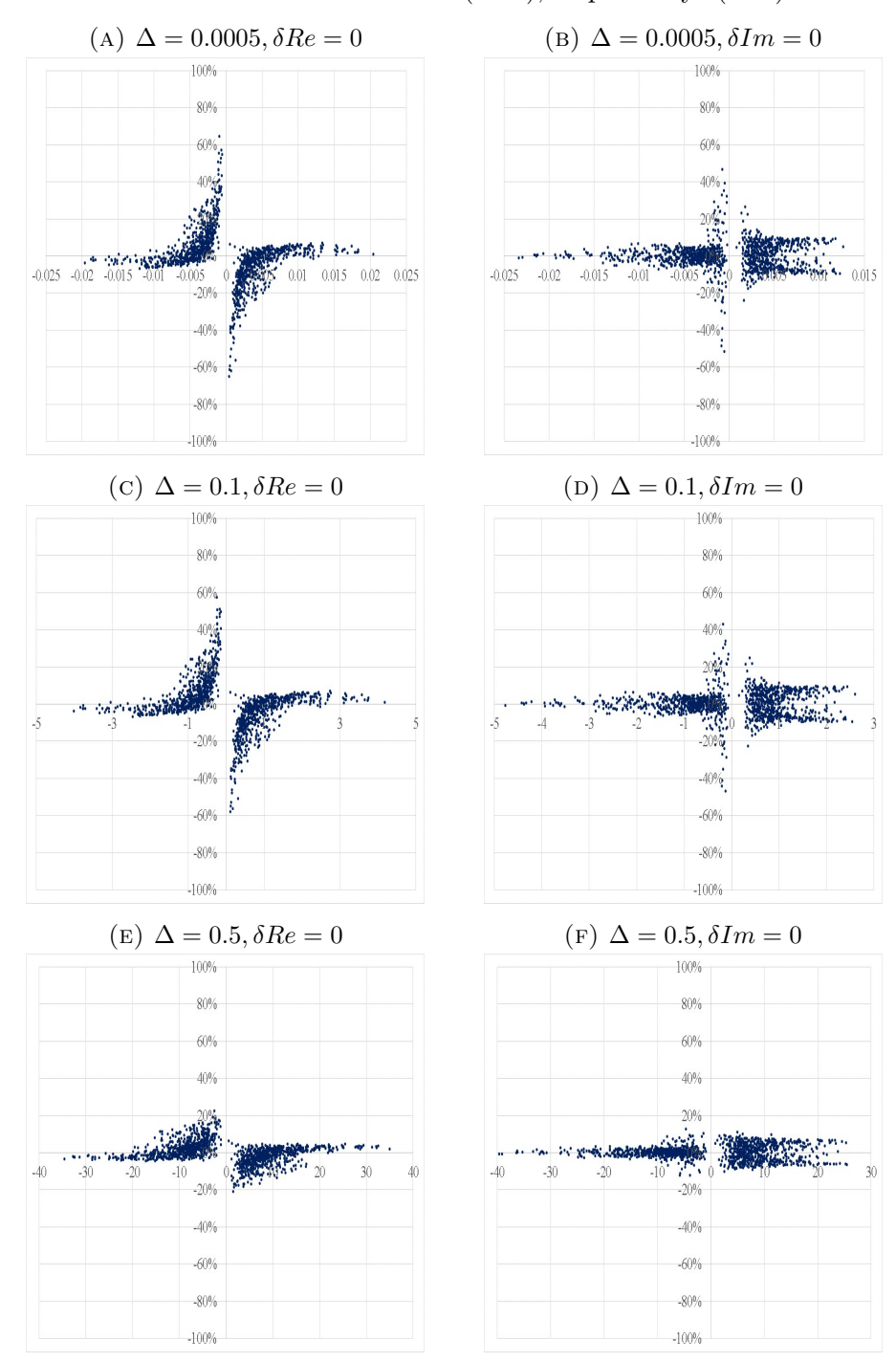
Developing on the previous subject, and in order to simplify the notations, let us pose first :

$$\delta Re = \delta Re(\Delta, t) = Re(\zeta(1/2 - \Delta + i.t)) - Re(\zeta(1/2 + \Delta + i.t))$$

$$\delta Im = \delta Im(\Delta, t) = Im(\zeta(1/2 - \Delta + i.t)) - Im(\zeta(1/2 + \Delta + i.t))$$

That done, it might be interesting to have a more precise view on the locus of the intersections of the real parts ($\delta Re=0$) between pairs of imaginary parts' intersections ($\delta Im=0$) and vice versa for the intersections of the imaginary parts ($\delta Im=0$) between pairs of real parts' intersections ($\delta Re=0$).

FIGURE 6. Distribution of $r(\delta Im)$, respectively $r(\delta Re)$.

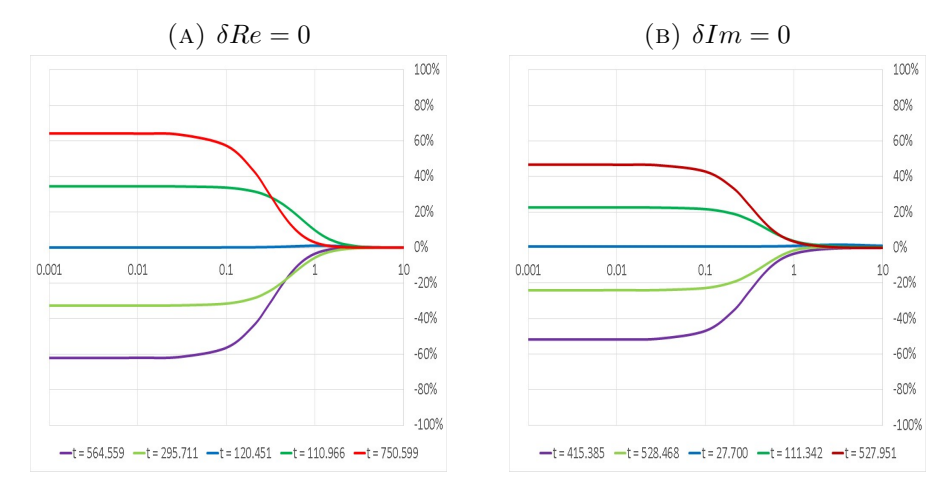


Let us consider the ordinates t_1 and t_2 ($t_2 > t_1$) of a pair of consecutive intersections of one color tone curves (blue for real parts and red for imaginary parts as illustrated in the figures 4A to 4D). We then calculate the locus of the ordinate t_3 the intersection of the intermediate intersections of the other color shade. We compute the difference $t_3 - \frac{t_1 + t_2}{2}$ that we compare to $t_2 - t_1$. In order to get a 100 % deviation if the ordinate t_3 is equal either to t_1 or t_2 , we add a multiplicative factor of 2 to the testing ratio getting in so doing $r = 2\frac{t_3 - \frac{t_1 + t_2}{2}}{t_2 - t_1}$. We draw that percentage choosing as abscissa δIm when we investigate the real parts' intersections ($\delta Re = 0$) and δRe when we investigate the imaginary parts' intersections ($\delta Im = 0$). The illustrations are given in figures 6A to 6F covering data within the interval $t \in [0, 1000]$.

Remarkably, the distributions are not normal distributions (and far from it in the case $\delta Im = 0$). However, most of the time, the higher the differences δIm , respectively δRe , the better the chances to have a small deviation to the middle expected ordinates. The exception is $\delta Im = 0$ and $\delta Re > 0$ where we observe an asymptotic limit range around $\pm 10\%$.

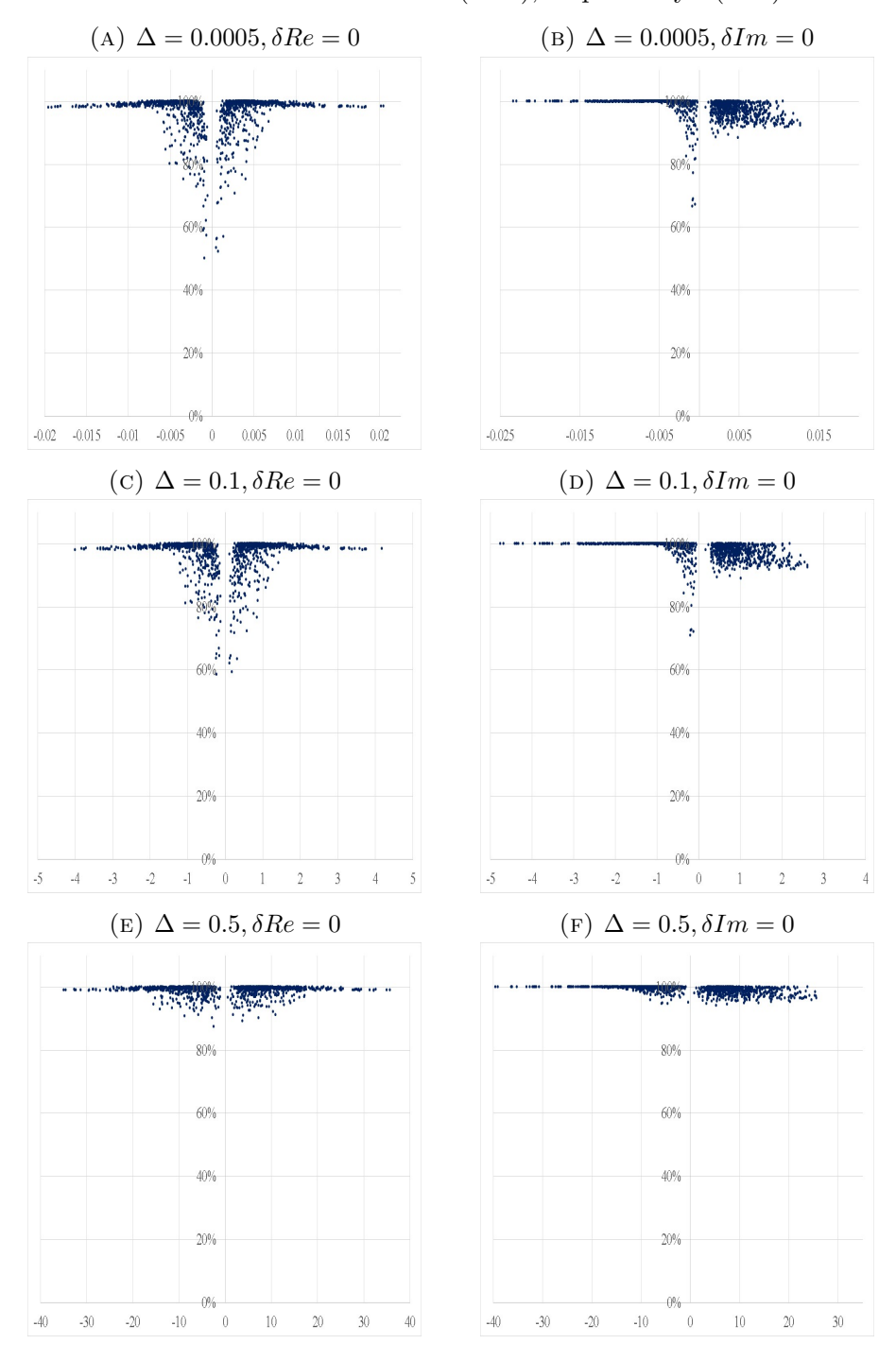
That said, for our part, what remains the most important is the confinement to the general $\pm 100\%$ range and that the distributions as a whole are getting systematically smaller in size as Δ increases (barely from $\Delta \approx 0$ to $\Delta \approx 1/10$ but much father so from thereon, the in-middle process being mostly completed when δ reaches approximately the value 2). A few sample is given in the figures 7A and 7B.

FIGURE 7. Evolution of $r(\delta Im)$, respectively $r(\delta Re)$, with Δ .



The illustrations given in figures 8A to 8F are constructed in a similar way. This time, we compute the ratio $h = \frac{\delta Im}{\delta Im_{max}}$, respectively $h = \frac{\delta Re}{\delta Re_{max}}$, where δIm_{max} , respectively δRe_{max} , are the corresponding local maximum values of $Im(\zeta(1/2-\Delta+i.t))-Im(\zeta(1/2+\Delta+i.t))$, respectively $Re(\zeta(1/2-\Delta+i.t))$

FIGURE 8. Distribution of $h(\delta Im)$, respectively $h(\delta Re)$.



 $(\Delta + i.t)$) – $Re(\zeta(1/2 + \Delta + i.t))$. We observe the same kind of exception as previously and the tightening of the distributions as Δ increases.

Note. One can be suspect of the later proof. Of course the distances between crossings and maximal spacings can be infinitesimal defying some arguments made. So let us recourse to an analytic proof inspired by the previous work but requiring no graphical support. Due to the difficulty of such task in the general context, we will add the legitimate supplementary condition which is that the four previous terms are not only equal but also equal to 0.

4. The analytic proof

Lemma 3. The function $\Xi(s) = \sum_{n=1}^{\infty} \frac{(-1)^{n-1}}{n^s}$ is analytic, thus infinitely derivable, within the domain of definition 0 < Re(s) < 1. Therefore $\Xi(s)$ and in particular its second derivative are well defined over that domain.

Proof. Using theorem 4, we get $\sum_{n=1}^{\infty} \frac{(-1)^{n-1}}{n^s} = (1-2^{1-s})\eta(s)$. The functions $\eta(s)$ and $(1-2^{1-s})$ are analytic over the said domain and so their product. In particular

$$\Xi''(s) = \sum_{n=1}^{\infty} \frac{(-1)^{n-1} \ln^2(n)}{n^s}$$

Lemma 4. The zeros of the function $\Xi(s)$ and $\zeta(s)$ are the same within the strict critical band.

Proof. We have $\sum_{n=1}^{\infty} \frac{(-1)^{n-1}}{n^s} = (1-2^{1-s})\eta(s)$. Therefore the zeros of $\Xi(s)$ are those of $\eta(s)$ plus those of $(1-2^{1-s})$, that is $\sigma=1$ and $t=2\pi k/ln(2)$, k an integer, and hence are outside the strict domain of definition. The functions $\eta(s)$ and $\zeta(s)$ have the same zeros in the mentioned domain, hence the lemma.

So, being only interested in the non-trivial zeros of the Riemann Zeta function, we can now simplify our task to merely solving $\sum_{n=1}^{\infty} \frac{(-1)^{n-1}}{n^s} = 0$. In order to have homogeneous notations, let us have

$$\Lambda_1(m, \sigma, t, \phi) = \sum_{k=1}^{m} (-1)^{k-1} k^{-\sigma} \sin(t \cdot \ln(k) + \phi)$$

and

$$\Lambda_2(m,\sigma,t,\phi) = \sum_{\substack{1 \le i \le m \\ 1 \le j \le m}}^m (-1)^{i+j} (i.j)^{-\sigma} \sin(t.\ln(i/j) + \phi).$$

Lemma 5. Solving $\sum_{k=1}^{m} \frac{(-1)^{k-1}}{k^s} = 0$ is equivalent to solving

$$\Lambda_1(m,\sigma,t,0) = \Lambda_1(m,\sigma,t,\frac{\pi}{2}) = 0.$$

Proof. $\frac{1}{k^s} = k^{-\sigma}k^{-i.t} = k^{-\sigma}e^{-i.ln(t)} = k^{-\sigma}(\cos(t.ln(k)) - i.\sin(t.ln(k))),$ hence the result after separating real and imaginary parts.

Lemma 6. Solving

$$\Lambda_1(m, \sigma, t, 0) = \Lambda_1(m, \sigma, t, \frac{\pi}{2}) = 0$$

is equivalent to solving

$$\Lambda_2(m,\sigma,t,\frac{\pi}{2})=0.$$

Proof. Using $\cos(a-b) \equiv \cos(a)\cos(b) + \sin(a)\sin(b)$, we get $(\Lambda_1(m,\sigma,t,0))^2 + (\Lambda_1(m,\sigma,t,\frac{\pi}{2}))^2 = (\sum_{k=1}^m (-1)^{k-1} k^{-\sigma} \sin(t.\ln(k)))^2 + (\sum_{k=1}^m (-1)^{k-1} k^{-\sigma} \cos(t.\ln(k)))^2 = \sum_{\substack{1 \le i \le m \\ 1 \le j \le m}} (-1)^{i+j} (i.j)^{-\sigma} \cos(t.\ln(i/j)) = \sum_{\substack{1 \le i \le m \\ 1 \le j \le m}} (-1)^{i+j} (i.j)^{-\sigma} \sin(t.\ln(i/j) + \frac{\pi}{2}) = \Lambda_2(m,\sigma,t,\frac{\pi}{2})$. Then $a^2 + b^2 = 0 \Leftrightarrow \{a = 0, b = 0\}$ allows to conclude.

Note. It is remarkable that the counterpart $\Lambda_2(m, \sigma, t, 0)$ of $\Lambda_2(m, \sigma, t, \frac{\pi}{2})$ is identically null, since $(-1)^{i+j}$ $(i.j)^{-\sigma}$ $\sin(t.\ln(i/j)) = -(-1)^{j+i}$ $(j.i)^{-\sigma}$ $\sin(t.\ln(j/i))$, which in some way also explains why only one equation subsides:

$$\Lambda_2(m, \sigma, t, 0) \equiv 0.$$

Lemma 7. The non-trivial zeros of the Riemann Zeta function are the zeros of

$$\sum_{\substack{1 \le i \le m \\ 1 \le j \le m}}^{m \to \infty} (-1)^{i+j} (i.j)^{-\sigma} \cos(t.\ln(i/j)) = 0$$

provided the proper convergence at the asymptotic limit.

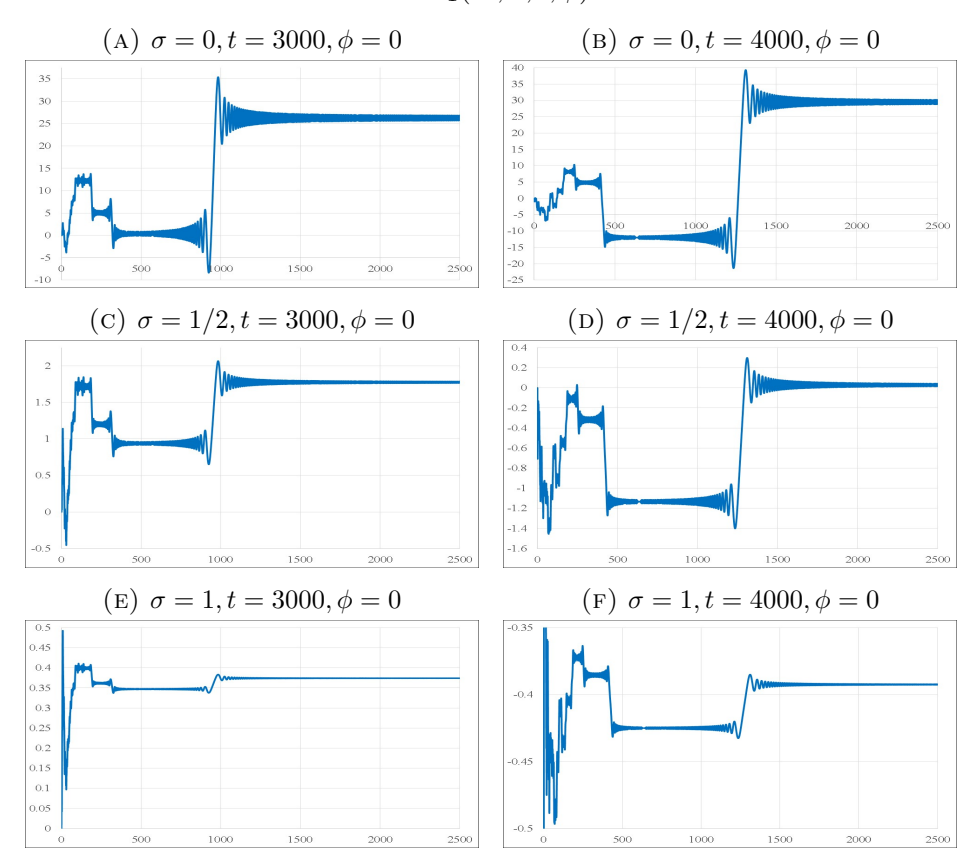
Proof. This is the immediate result of the former lemmas. \Box

Lemma 8. Let us have some given values $\sigma \in]0, \infty[$ and t > 0. The expression $\Lambda_2(m \to \infty, \sigma, t, \frac{\pi}{2})$ is a semi-convergent series. The truncations at rank m give acceptable approximations of the value of the infinite sum for m > t.

Proof. For $m \to \infty$, the functions $\Lambda_1(m,\sigma,t,0)$ and $\Lambda_1(m,\sigma,t,\frac{\pi}{2})$ identify, via lemma 4, with the real and imaginary parts of $(1-2^{1-s})\eta(s)$ an analytic function. So the functions $\Lambda_1(m,\sigma,t,0)$ and $\Lambda_1(m,\sigma,t,\frac{\pi}{2})$ are semi-convergent. The finite sum (so in particular the sum of two functions) of semi-convergent functions is semi-convergent. The square of a semi-convergent function is semi-convergent (see reference [17]). Therefore $\Lambda_2(m,\sigma,t,\frac{\pi}{2})$ is semi-convergent recalling that we use the same trivial order m for $\Lambda_1(m,\sigma,t,\phi)$ and $\Lambda_2(m,\sigma,t,\phi)$ as we add progressively terms to the sums.

The graphics in figures 9A to 9F are typical of the way the values of Λ_1 evolves as m increases. It shows sudden jumps in values that may seem random. Therefore, it is advisable to trace the origin of these jumps, in order

FIGURE 9. Evolution of $\Lambda_1(m, \sigma, t, \phi)$ versus m.



to discard any useless doubts. The function Λ_1 is not a systematic alternating sum. A jump results visually, at some stage, from enough successive terms of same sign. Within the series' term $(-1)^{i-1}$ $i^{-\sigma} \sin(t.\ln(i) + \phi)$, the term $i^{-\sigma}$ has no effect on the change of sign. It remains therefore $(-1)^i \sin(t.\ln(i) + \phi)$. Multiple terms of same sign starts with at least two successive terms. For two same sign successive terms, it is sufficient asymptotically to have $(-1)^i \sin(t.\ln(i) + \phi) \approx (-1)^{i+1} \sin(t.\ln(i+1) + \phi)$. From that, we deduce $\sin(t.\ln(i+1) + \phi) \approx -\sin(t.\ln(i) + \phi)$, or $\sin(t.\ln(i+1) + \phi) \approx \sin(\pi + t.\ln(m) + \phi)$, and then $t.\ln(i+1) \approx (1+2k).\pi + t.\ln(i)$, or finally

$$\frac{t.ln(1+\frac{1}{i})}{\pi} \approx 1 + 2k$$

where $k \in \mathbb{Z}$.

For t > 0 and i > 0, k is necessarily in N.

When $i \to +\infty$, and t has some given value, the expression $t.\ln(1+1/i)/\pi \to 0$, so that, considering the order 0 < 1 < 1 + 2k if k > 0, the value of m for which $t.\ln(1+1/m)/\pi \approx 1$ is the last one for which a jump occurs. The

initial expression will start to converge towards its asymptotic value after this last leap which intervenes therefore at rank

$$m \approx \frac{1}{\exp(\frac{\pi}{t}) - 1}$$

In the case of the graphics in figure 9, we have $m \approx 1/(exp(\pi/3000) - 1) \approx 954$ and $m \approx 1/(exp(\pi/4000) - 1) \approx 1273$ which are right on spot of the values obtained numerically. The other jumps occur around the ranks m such as

$$m_k \approx \frac{1}{\exp(\frac{(1+2k)\pi}{t}) - 1}$$

This gives Table 1. This table shows that we still get jumps right on spot

Table 1

t = 3000t = 4000k m_k m_k 5 86 115 4 106 141 3 136 181 2 190 254 1 424 318 0 1273 954

Table 2

	t = 3000	t = 4000
k	n_k	n_k
5	95	127
4	119	159
3	159	218
2	238	318
1	477	636
0	∞	∞

where they are expected. But as one gets down towards smaller ranks m, the "randomness" will take over completely in the numerical results.

This allows to give the lower bound approximate rank m_{asymp} , for some t, to get a fair asymptotic evaluation. Typically, one can choose twice the rank of the last jump

$$m_{asymp} \approx 2 \frac{1}{exp(\frac{\pi}{t}) - 1}$$

or approximately, as soon as $t \gg \pi$,

$$m_{asymp} \approx \frac{2t}{\pi} \approx 0.64 \ t$$

Now, when we are interested in areas where the function studied is not subject to a jump, but is rather close to a zero slope, the equation to be solved is $(-1)^i \sin(t.\ln(i)) \approx -(-1)^{i+1}.\sin(t.\ln(i+1))$ and therefore, for $k \in \mathbb{Z}$,

$$\frac{t.ln(1+\frac{1}{i})}{\pi}\approx 2k$$

The corresponding ranks n_k for the plateau zones are

$$n_k \approx \frac{1}{exp(\frac{2\pi k}{t}) - 1}$$

So that, for our examples, we get table 2.

The same truncation m will be adequate for $\Lambda_2(m, \sigma, t, \frac{\pi}{2})$.

Lemma 9. The expression $\Lambda_2(m \to \infty, \sigma, t, \frac{\pi}{2})$ is positive or null.

Proof. The expression is a sum of two real value squares. \Box

Lemma 10. Let us have for some variable σ and a given fixed choice of real value t and positive integer m

$$\tau(\sigma) = \sum_{\substack{1 \le i \le m \\ 1 \le j \le m}} a_{i,j} (i.j)^{-\sigma}$$

where

$$a_{i,j} = (-1)^{i+j} \cos(t \cdot \ln(i/j)).$$

Then $\tau(\sigma)$ has at most one and only one zero over σ in $]0,\infty[$.

Proof. The function $\tau(\sigma)$ is identical $\Lambda_2(m, \sigma, t, \frac{\pi}{2})$. Hence it is positive or null. We use that alternative in order to avoid a cumbersome notation underneath as we are only interested on the evolution of the function while varying σ . Let us have

$$\tau(\sigma) = \tau_{+}(\sigma) + \tau_{-}(\sigma)$$

where

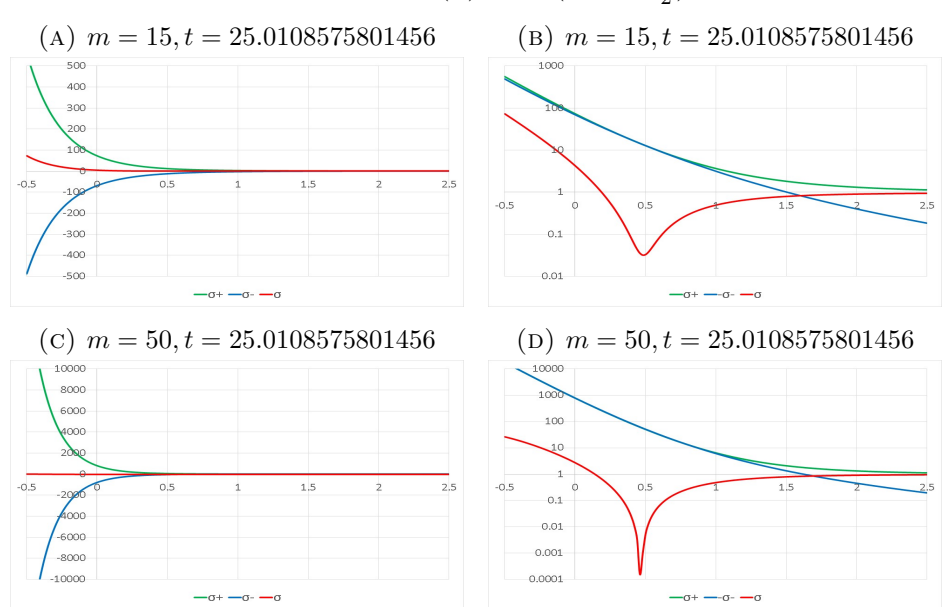
$$\tau_{+}(\sigma) = \sum_{\substack{1 \le i \le m, \ 1 \le j \le m \\ a_{i,j} > 0}} a_{i,j} (i.j)^{-\sigma}$$

and

$$\tau_{-}(\sigma) = \sum_{\substack{1 \le i \le m, \ 1 \le j \le m \\ a_{i,j} < 0}} a_{i,j} (i.j)^{-\sigma}.$$

Each term of $\tau_{+}(\sigma)$ is positive and each term of $\tau_{-}(\sigma)$ is negative. The second derivative of $\tau_{+}(\sigma)$, respectively $\tau_{-}(\sigma)$ (versus σ) are obtained by multiplying each term of the sum by $ln^2(i,j)$ which has no effect on the sign of the addends. Therefore $\tau_{+}(\sigma)$ has a positive second derivative over all of]0,1[while $\tau_{-}(\sigma)$ has a negative second derivative over all of]0,1[. Therefore three possibilities arise. Either the trajectories of $\tau_{+}(\sigma)$ and $\tau_{-}(\sigma)$ don't cross, cross exactly at two points or at one point. Remember these trajectories are drawn for some given value t (and m). In the first case, it means that we chose an ordinate t without any crossing solution which is the standard expected result for a random choice (of t). Envisaging the second case, with an adapted choice of t, would mean that $\tau(\sigma)$ is negative for the range of abscissa σ between the two distinct points of intersections of the trajectories $\tau_{+}(\sigma)$ and $\tau_{-}(\sigma)$. This cannot happen as the function $\tau(\sigma)$ is positive or null. The third case, with one unique tangential common point, is therefore the only one available when the trajectories $\tau_{+}(\sigma)$ and $\tau_{-}(\sigma)$ do share some coordinates.

FIGURE 10. Evolution of $\tau(\sigma) \equiv \Lambda_2(m, \sigma, t, \frac{\pi}{2})$.



A sample of the trajectories is given in the figures 10A to 10D illustrating the 3^{rd} Zeta function's zero. The ordinates' scale in the left side's graphics is the standard linear scale while it is logarithmic in the right side's graphics in order to highlight the approximate zero. We choose two values for m. For small values of m, before the final convergence is initiated, there is no reason to even see for $\tau(\sigma)$ a trajectory in the form of a potential well at some σ . (It would be the case here for $m \leq 10$). We meet the final convergence threshold for this example with the small rank m = 15 (as $15/t \approx 15/25 = 0.6$). As m increases further, the trajectory of $\tau(\sigma)$ varies little while, on the contrary, $\tau_+(\sigma)$ and $\tau_-(\sigma)$ increase in absolute values fast at abscissas $\sigma << \frac{1}{2}$.

Note. The domain is which the previous arguments are true is larger than]0,1[. However one cannot use it in order to address any property or data relative to $\zeta(s)$ on the left side of that domain. We extended the graphics to [-1/2,5/2] on the sole purpose to get a broader view on the evolution of the trajectories.

Lemma 11. The trajectories of $\tau_{+}(\sigma)$ and $\tau_{-}(\sigma)$ share one tangential point at most asymptotically.

Proof. As $m \to \infty$, the functions $\tau_+(\sigma)$ and $-\tau_-(\sigma)$ tends towards the same trajectories around the eventual common point. Asymptotically, as the trajectories flatten, either the trajectories $\tau_+(\sigma)$ and $-\tau_-(\sigma)$ are the same line, so that $\tau(\sigma) \equiv 0$, which is absurd as clearly $\tau(\sigma) \equiv \Lambda_2(m \to \infty, \sigma, t, \frac{\pi}{2})$ is

not identically null, or the unique point intersection subsides, as it is the only authorized option (in case of intersection) for any $m \in N$.

Theorem 8. The Riemann hypothesis is true.

Proof. For some given t, the function $\Lambda_2(m \to \infty, \sigma, t, \frac{\pi}{2})$ can take at most one value σ for which it cancels according to lemma 11. By the symmetry of the Zeta function's zeros imposed by theorem 5, which zeros when they exist are therefore located on the same ordinate t, that unique cancellation over the interval $\sigma \in]0,1[$ can only occur on the critical line.

Note. The symmetry imposed by theorem 5 doesn't apply, by the result obtained above, to the trivial zeros of $\zeta(s)$ as their locus is outside the critical line on its left side where $\eta(s)$ and $\zeta(s)$ do not match at all.

5. The complex plane graphical context

5.1. The standard context. The Riemann Zeta function is an odd function in regard to the t ordinate. Therefore, our study will be focused on the positive values of that variable, once for all.

Lemma 12. Let us consider two oriented parallel vertical segments in the complex plane s and $s + \epsilon$ where $s = \sigma + i.t$, σ has some fixed value, ϵ is a real valued infinitesimal and $t \in [t_1, t_2]$, $0 < t_1 < t_2$. The rectangular section between the two segments does not contains the pole of the Zeta function (because t > 0). Then the oriented images, obtained by applying the Zeta function, to these lines stay on the same side one in regard to the other. For a line on the right side of its neighbour, its image is on the right side of its neighbour's image also.

Proof. This results from the fact that the ζ -function is analytic (except at the pole). Therefore, locally according to theorem 2, for a small enough region of the domain, it provides a bijective conformal map from the domain to the codomain except if the domain contains a zero of the first derivative (or the pole). The zeros of the first derivative (function which is analytic also) are isolated zeros by theorem 1 and therefore the preceding argument holds in any sufficiently infinitesimal domain near but not containing the zero. Considering two parallel oriented lines in that region, the composition by the Zeta function provides two oriented lines in the codomain which do not cross. Of course, by extending the domain, the bijection at some step will eventually fail.

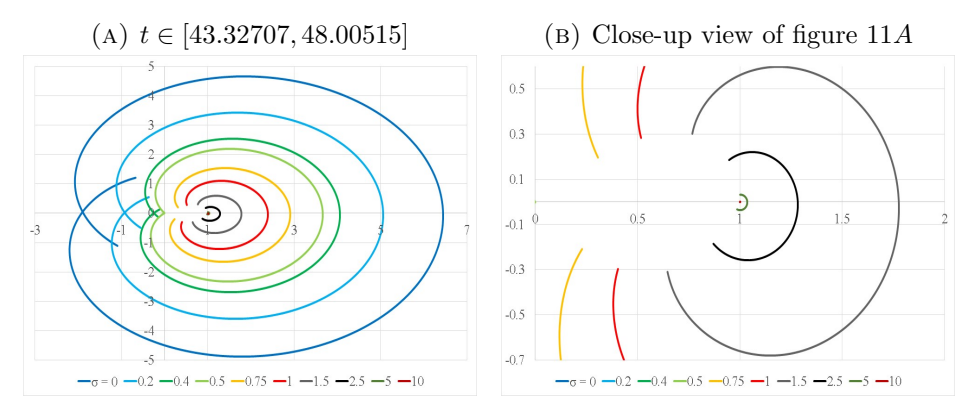
The respective side in the image for some given respective side in the domain being necessarily always the same according to the first part of this proof, a numerical example enables to conclude immediately that right side provides right side (and left provides left).

Let us then consider the complex plane domain $t \in [t_1, t_2]$ where t_1, t_2 are the imaginary parts of two successive non-trivial positive zeros of the Zeta function, choosing here expressly zeros with real part value 1/2. The

image of the continuous network of vertical segments of that domain by the Riemann Zeta function provides a continuous network of curves that divides a priori into two types of configurations.

The first one derives from the absence of a zero of the first derivative of the Zeta function in the chosen domain. The second one derives from the presence of one and only one zero of the first derivative of the Zeta function at some abscissa σ greater than 1/2.

FIGURE 11. Trajectories $\zeta(\sigma + i.t)$ for constant σ

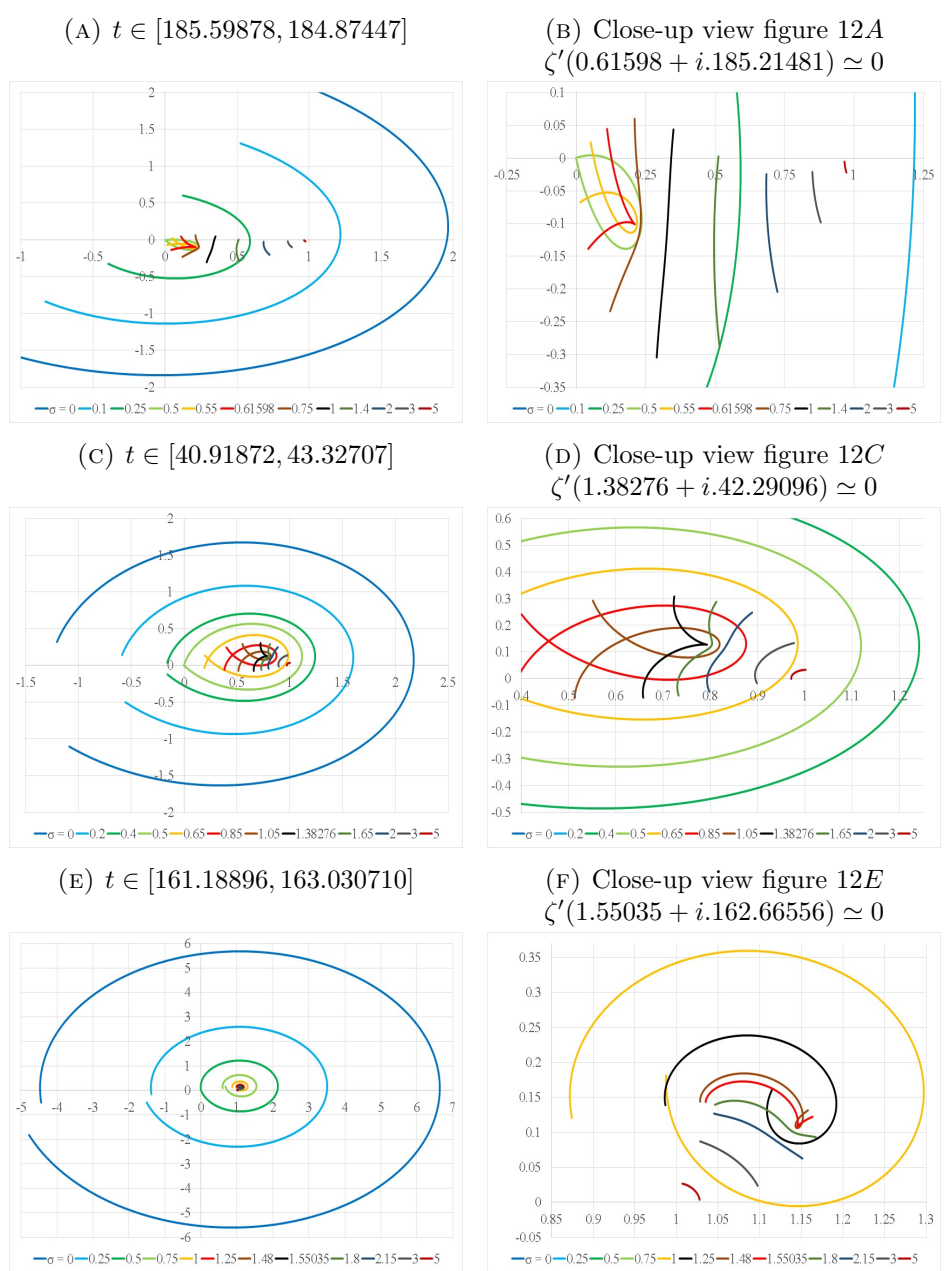


To gather these two kind of drawings, it suffices to consider a rectangular domain $\sigma \in [\sigma_1, \sigma_2]$ and $t \in [t_1, t_2]$ where for example $\sigma_1 = 0$ or some finite sufficient lesser value and $\sigma_2 = 5$ or some finite sufficient greater value.

Before distinguishing the two configurations, let us start by noting the common feature. There is a progressive evolution from a large scale image for "large" negative values of σ to minute forms for "large" positive values of σ , the later forms converging to the coordinate (1,0). The exponential evolution results from the $\frac{1}{n^{\sigma}}$ contribution of each of the Riemann Zeta function terms. It leads, and that is seen clearly on any sample, to a rapid reducing scaling effect. Figures 11 and 12 are such samples as σ is given higher values while keeping the same sized vertical segments in the domain. The image of two infinitesimal close segments shift progressively on the same side in the absence of a zero of the derivative within the domain and therefore the image will head asymptotically to the coordinate (1,0) as illustrated by figures 11A and 11B, this example being the first and simplest type of configuration, the case where, let us say abruptly, nothing special happens.

The second type is produced when $\zeta'(s) = 0$ for some coordinate s within the chosen wide enough rectangular domain. Supposing any such event, we get the examples of the figures 12A to 12F. Here the conformal map argument holds for the image of the left part of the rectangular domain up to the abscissa of the zero of the derivative on one hand and again separately for the image of the right part of rectangular domain starting at the abscissa of the said zero of the derivative on the other hand. This time,

FIGURE 12. Trajectories $\zeta(\sigma + i.t)$ for constant σ



the exponential reducing trend may be false locally. Indeed, by definition, $\zeta(s+\epsilon)-\zeta(s)\to \zeta'(s).\epsilon$ as $\epsilon\to 0$ and therefore the distances $\zeta(s+\epsilon)-\zeta(s)$ are locally shorter near the image's locus where $\zeta'(s)$ is small, including thus the case $\zeta'(s) = 0$. Therefore, the same way that there is logic for a reduction of size of the images before the event $\zeta'(s) = 0$, there is no surprise for eventually an increase of the lengths of the vertical lines' images after that event is crossed (see for example figure 12B where that occurs between $\sigma \approx 0.616$ and $\sigma \approx 1$). The effect is much more visible if one reduces the domain to a smaller height band which still includes the zero of the derivative.

Note. The lemma is also true when the oriented parallel segments are not vertical.

Note. For the first type of configuration, in the absence of "disturbance" by a zero of the derivative, all curves shifting on the same side to each other, there exists only the double intersection solution, among all image's segments on the right side of the critical line, this line included, with the (0,0) coordinate which results from the initial choice of the two successive zeros on the said critical line. No intersection for the strict right side means, as we know, no intersection also on the strict left side neither, thus the Riemann hypothesis confirmation for this first case.

For the second type of configuration, the remarks are quite analogous but the arguments in favour of the Riemann hypothesis are trickier to explicit and somewhat opposable in the case of the existence of a zero of the derivative with abscissa lesser than 1/2. Indeed, one can recall the Speicher's theorem which confirms the Riemann conjecture's if $\sigma > 1/2$ for all Zeta function derivative's zeros (see reference [4]).

The two configurations being presented, let us frame it more precisely, in regard to the Riemann hypothesis, balancing between shortcomings or plausibility.

Let us consider the figure 1. If the Riemann hypothesis is true, as t increases, each loop formed by the trajectory of $\zeta(0.5+i.t)$ will exactly cross one time the (0,0) coordinate. If the Riemann hypothesis is false, as t increases, the trajectory of $\zeta(0.5+i.t)$ will necessarily be short of the intersection with (0,0) and, because of the pairing of the zeros expressed in theorem 5, the same trajectory will also experience an overdrive of the coordinate (0,0). The typical graphical result, for that piece of the trajectory, of that constrain is represented in figure 13A. Of course, the short shot and the overdrive may not be consecutive. There can be one or more loops, in-between these two events, intersecting with (0,0), but these cases would not change in any way the arguments coming next. Indeed, the typical trajectories for $\zeta(0.5 - \Delta + i.t)$ and $\zeta(0.5 + \Delta + i.t)$, $\Delta > 0$, corresponding to intersections with (0,0), are then represented in figure 13B. Their respective evolutions, as σ evolves from 0.5 to 0.5 - Δ and from 0.5 to 0.5 + Δ , result from lemma 12 that we will prove later on. In figure 13B, the intersections of these first and second trajectories with (0,0) can be in reverse pointed back to the ordinates t1 and t2 respectively on the $\zeta(0.5+i.t)$ trajectory, the red arrows being a help to indicate the said ordinates. The relevant ordinates are, of course, shown in a very approximative way here. However, these ordinates t1 and t2 are necessarily distinct on the trajectory $\zeta(0.5+i.t)$

which contradicts theorem 5, the later compelling to their equality. Hence the Riemann hypothesis should not be false.

Note. One of the variant to the figure 13A is that the overdrive happens before the short shot of (0,0). In this case it would result to a simple reversal of the direction of the y-coordinates to restore the same pattern. It wouldn't change any thing to our previous arguments.

Note. To be truly exhaustive, we have to prove also that the trajectory $\zeta(\sigma+i.t)$, σ being some constant, consists of loops that always occur always in a clockwise manner, as t increases, a point that we will address in the proofs of lemmas 14 and 18. Otherwise alternative designs to the one in figure 13A may be proposed with a risk they won't meet all the previous arguments.

Note. The scaling of the figure 13B (and figure 13A) is absolutely arbitrary. Therefore the difference t2 - t1 can be arbitrary small. That makes it so difficult to prove the Riemann hypothesis in any other way.

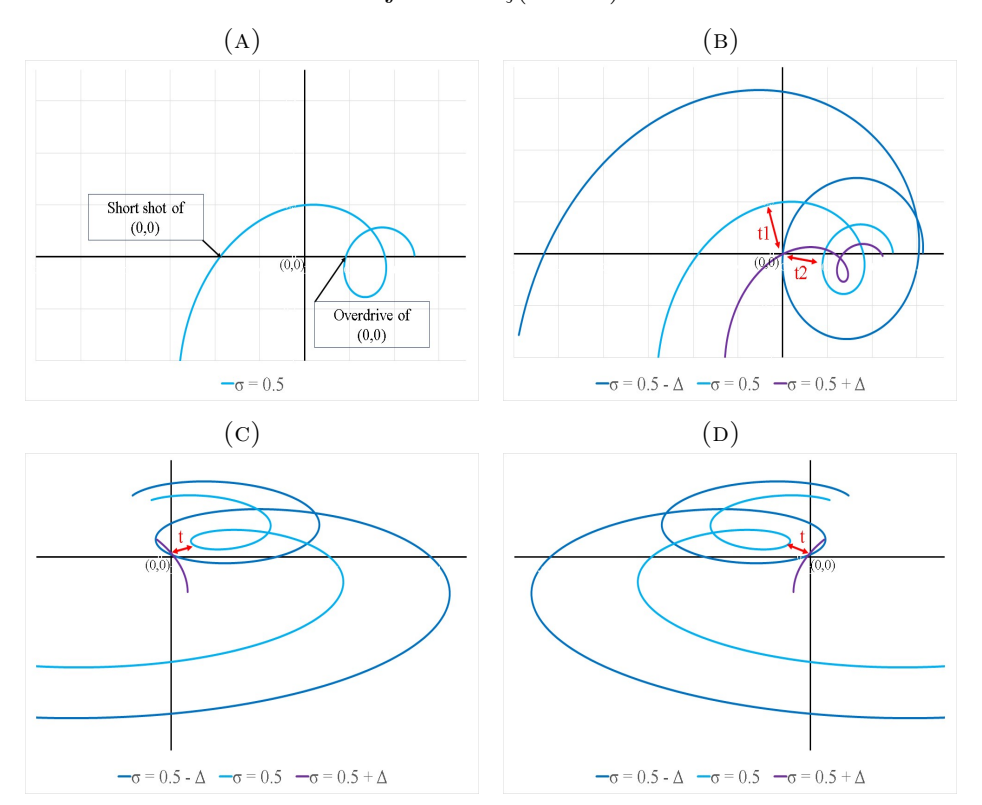


FIGURE 13. Trajectories $\zeta(\sigma + i.t)$ for constant σ

All these arguments don't however resist to the graphics proposed in figures 13C and 13D in which we simply position the blue loop (where $\sigma =$

1/2) at a more challenging place. Of course, figure 13C is not likely, because when σ increases, $\zeta(s)$ would head towards the coordinate (1,0) instead of (0,0) (that is towards the right direction instead of keeping its left direction as suggested in the graphic) as soon as the loop vanishes. Similarly figure 13D is not much more plausible, because it supposes a positioning of the "center" of the blue loop at the left of the y-axis which numerical examples never show (it would likely mean that $\zeta'(s) = 0$ for some $\sigma < 1/2$). Although none of these two latest examples match an expected design, referring to the standard configurations, we can't just affirm that it can't happen. More arguments are needed here to confirm the Riemann hypothesis.

5.2. Understanding the standard context. Let us consider the domain of vertical lines of positive ordinates and apply the Riemann Zeta function from large negative abscissas σ up to large positive values of that variable.

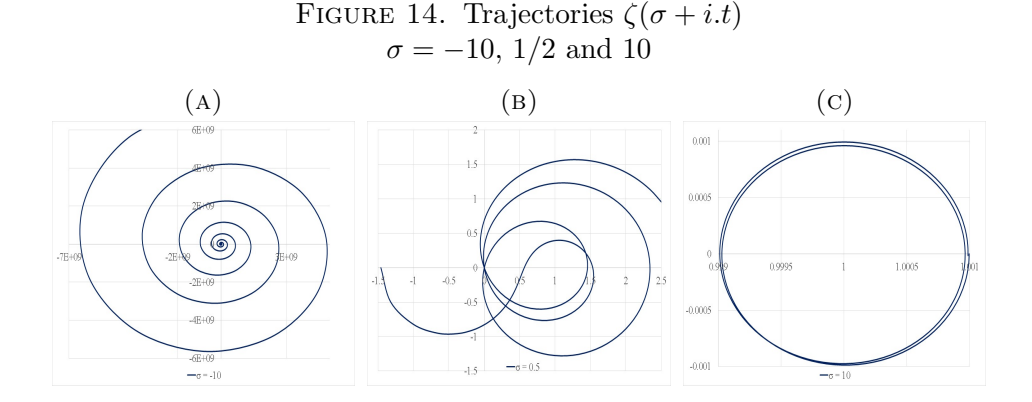
Lemma 13. The image of a positive oriented vertical half line $s = \sigma + i.t$, $\sigma << 0$, t > 0, by the zeta function, consists of an approximative outwards logarithmic spiral clockwise trajectory around the (1,0) coordinate. The image of a positive oriented vertical half line $s = \sigma + i.t$, $\sigma >> 1$, t >> 10, by the zeta function, consists of an approximative circular clockwise trajectory around the (1,0) coordinate.

Proof. As σ tends towards $+\infty$, comparing the results corresponding to two constant such σ , the term $\frac{1}{2^s}$ is getting rapidly preponderant in $\zeta(s)-1=\sum_{n=2}^\infty \frac{1}{n^s}$. This term is equal to $2^{-\sigma}(\cos(\ln(2).t)-i.\sin(\ln(2).t)$ and thus provides a circular trajectory of periodicity $\Delta t = \frac{2\pi}{\ln(2)}$, oriented clockwise, hence the resulting approximate circle trajectory for the whole sum. A numerical check shows that the approximation is satisfactory (for our purpose) as early as $\sigma > 10$. The sum $\sum_{n=3}^\infty \frac{1}{n^s}$, in the same way, for high value of σ , has preponderant term $\frac{1}{3^s}$. Therefore solving $\sum_{n=2}^\infty \frac{1}{n^{s1}} = \sum_{n=2}^\infty \frac{1}{n^{s2}}$, $s_1 \neq s_2$, is pretty much solving the approximation $\frac{1}{2^{s1}} + \frac{1}{3^{s1}} \approx \frac{1}{2^{s2}} + \frac{1}{3^{s2}}$, hence consists in getting a crossing of the circle $\frac{1}{2^{s1}}$, which trajectory experienced a perturbation by the additional much smaller term $\frac{1}{3^{s1}}$, with the same kind of shifted trajectory. It is obvious that a progressive shifting of the value of s_2 will provide such crossing event quite soon. That shifting of s_2 can be repeated at will, thus the infinity of self-crossings of the trajectory for large constant values σ as t increases to infinity.

As σ tends towards $-\infty$, the zeta function is getting way off the values (and trajectories) of the sum $\sum_{n=1}^{\infty} \frac{1}{n^s}$. However, taking the Euler-Maclaurin summation [5] for its analytic continuation, the various terms containing n^{-s} still confirm the divergence observed in the original sum thanks to the $n^{-\sigma}$ corresponding parts while spiralling due to $n^{-I.t}$ components. It results in an outwards clockwise logarithmic-like trajectory at constant σ and positive t increasing values. The divergence of that trajectory will be faster as the absolute value of σ is chosen greater. Contrary to the preceding case,

no self-crossing of the trajectory can occur in these conditions. The approximation is plainly satisfactory (for our purpose) as early as $\sigma < -10$. The figures 14A and 14C underneath illustrate the two preceding cases. In the second instance there are self-crossings of the trajectory while in the first one there are none.

Note. The (1,0) coordinate, we refer in this lemma is not of course the pole as we are in the codomain instead of the domain of the function.



Note. In a nutshell, for a domain consisting in vertical half-lines of positive ordinate and abscissa increasing from (almost) $-\infty$ to $+\infty$, the initial part of this article will be to tell the story of the contraction of their successive continuous images from the infinite spiral in figure 14A down to the figure 14C. It consist in the progressive building of an infinite number of local loops which sizes get smaller and smaller until vanishing and a residual infinite number of loops which head towards the unique point (1,0). In particular, the story will show that loops don't pop up suddenly but are only the result of the said contraction. This is coherent only if all loops are oriented in the same way as we will assess now.

5.2.1. Adding oriented circles.

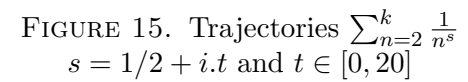
Lemma 14. Let us consider a positive oriented vertical segment in the complex plane $s = \sigma + i.t$, with $\sigma > 1$, $t \in [t_1, t_2]$ and its image $\zeta(s)$. Then every closed loop within the image can only be fully completed clockwise (i.e. on a right-side trajectory).

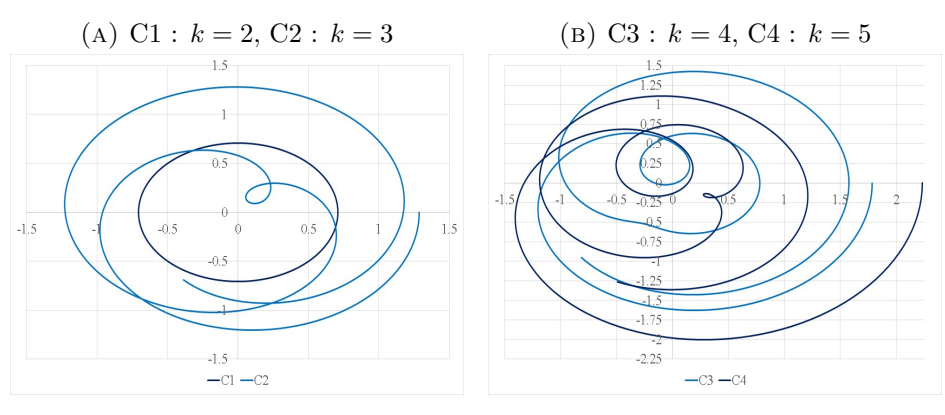
Proof. (1). For $\sigma > 1$, we get by definition

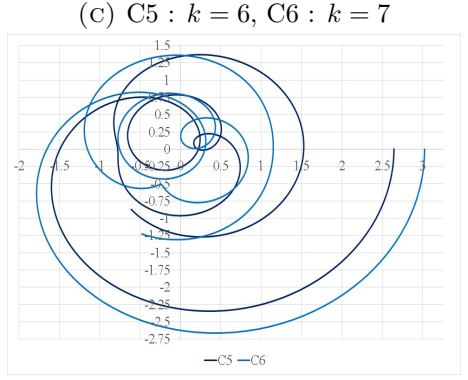
$$\zeta(s) - 1 = \sum_{n=2}^{\infty} \frac{1}{n^s} = \sum_{n=2}^{\infty} n^{-\sigma} (\cos(\ln(n).t) - i.\sin(\ln(n).t)).$$

Each term of the series describes the trajectory of a circle of radius $n^{-\sigma}$ with centre (0,0) in the complex plane and periodicity $\frac{2\pi}{\ln(n)}$. The function

 $\zeta(s)-1$ is locally a sum of partial circles all with the same centre and same clockwise orientation, and $\zeta(s)$ is obtained with a simple unit shift of abscissa of the resulting sum maintaining trivially the same trajectory shape. To get a clockwise trajectory by adding clockwise circles shouldn't come as a surprise. Additional arguments are however welcome. In order to prove the lemma, let us proceed by induction. Figures 15A to 15C confirm the lemma for the initial step, being a trivial circle, and some additional cases. The value of σ is sparsely relevant as it is only a scaling factor in the present argument, thus it doesn't matter to take it here equal to 1/2, instead of greater then 1, as we did in the figures. These initial examples provide a sample of curves with the said clockwise loops and the last figure shows also an example of an "aborted" loop with a "cusp-like" silhouette. Of course, it is only cusp-like, but it is never a cusp, as the sum of analytic function terms, here $\frac{1}{n^s}$, is analytic.



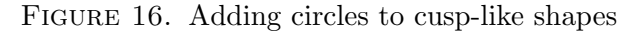


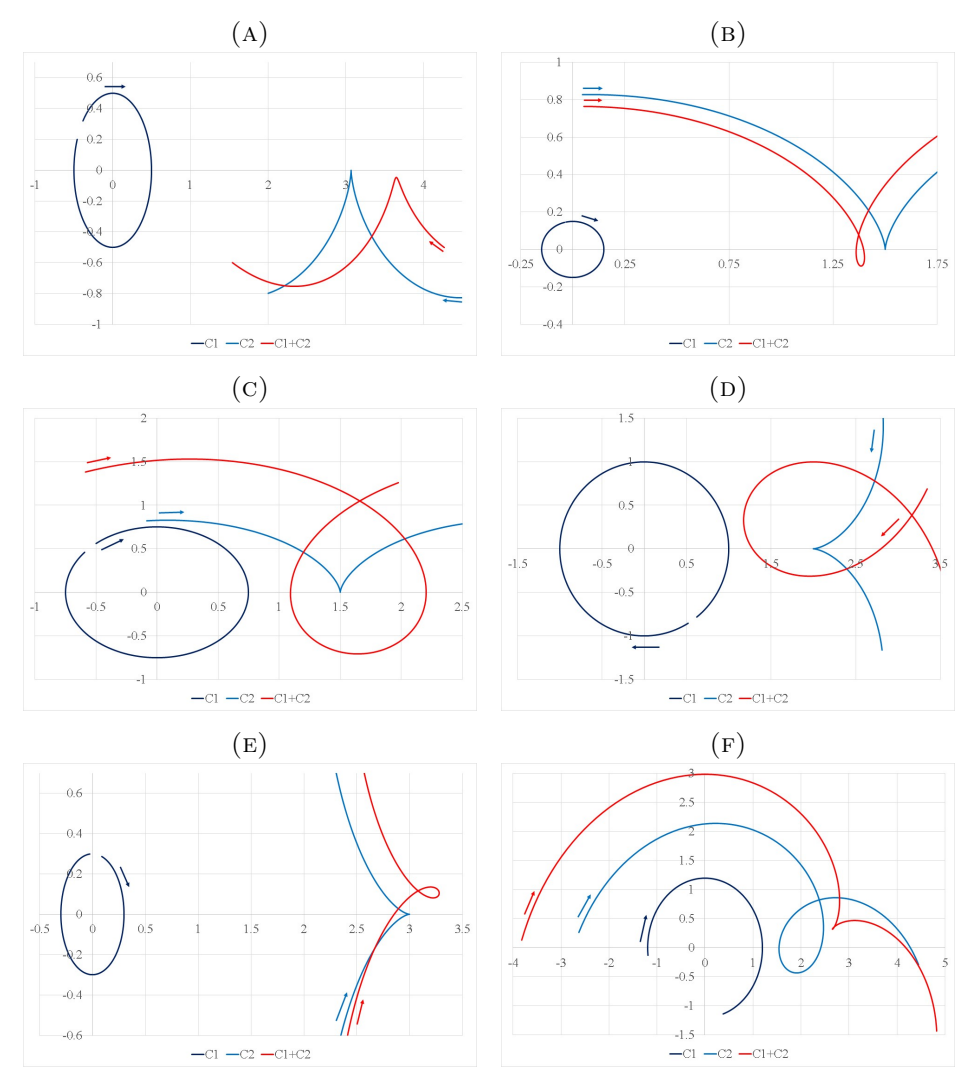


Let us suppose then, for $\sum_{n=2}^{j} \frac{1}{n^s}$, the lemma true at some given step j. We then consider the sum $\lambda \frac{1}{(j+1)^s} + \sum_{n=2}^{j} \frac{1}{n^s}$ with $\lambda \in [0,1]$. As we increase λ from 0 to 1, we pass from the case j to the case j+1. Examining the

change of the trajectory as we increase λ , after a smooth evolution, one or more loops will eventually pop up with infinitesimal sizes, for let say the value $\lambda = \lambda_0$, before growing further. This popping-up can occur only at the bottom of the cusp-like silhouettes because of the cusp-like geometry at that precise spot (the function being analytical, again, no truly cusp can occur there) and will then grow to provide examples like those displayed in figures 16B to 16E. Depending on the corresponding phase value of the circle at the cusp-like bottom, instead of a loop, the sum with the cusp-like trajectory may give, like in figure 16A, a wider open trajectory. This kind of cases is of no peculiar need to be addressed and therefore disregard in the further development of the present argument. As $(\lambda_0 + \epsilon) \frac{1}{(j+1)^s}$ is added to the sum $\sum_{n=2}^{j} \frac{1}{n^s}$, for infinitesimal ϵ , the one or more nascent loops in the resulting trajectory are necessarily on the same side as the bottom of the cusp-like silhouette as shown in the figures with the loops' orientations as indicated by arrows. As this bottom was on the right hand side of the trajectory at step j, it will be likewise at that stage. As λ grows further, the general direction of the axis of "symmetry" of the loop and its size may vary but as long as the loop keeps close it will remain clockwise as the different resulting trajectories can't cross locally according to lemma 12. The three figures 16B to 16D display standard trajectories. This is not the case of figure 16E which is the result of a loop popping-up within a larger loop, thus the bottom of the silhouette is oriented to the opposite side in regard to the complex plan centre (0,0). Note that all these figures are not extracted from real cases of the zeta co-domains but do however reflect them. We can express the previous argument in plain equations. We use the conventional writing if(a,b,c) which means if a is true then b else c. Choosing new orthonormal axis with an adapted angle to the usual complex plane axis, the threshold cusp-like trajectory can be written down as two pieces of circles $if(t < t_{00}, \sigma_1 + i.t_1 + r_1(cos(\alpha_1.t + \phi_1) - i.sin(\alpha_1.t + \phi_1)),$ $\sigma_2 + i \cdot t_2 + r_2(\cos(\alpha_2 \cdot t + \phi_2) - i \cdot \sin(\alpha_2 \cdot t + \phi_2)))$, the first of centre (σ_1, t_1) and radius r1, the second of centre (σ_2, t_2) and radius r2 with both coefficients α_1 and α_2 positive and t_{00} the value of t at the "cusp". Joining them at (σ_0, t_0) at the end for the first one and at the beginning for the second one, we get the series of equalities $\sigma_0 = \sigma_1 + r_1 \cdot \cos(\alpha_1 \cdot t_{00} + \phi_1) = \sigma_2 + r_2 \cdot \cos(\alpha_2 \cdot t_{00} + \phi_2)$ and $t_0 = t_1 - r_1.\sin(\alpha_1.t_{00} + \phi_1) = t_2 - r_2.\sin(\alpha_2.t_{00} + \phi_2)$. The centres of the circles being aligned with (σ_0, t_0) , we have also $r_2 = -\frac{\sigma_2 - \sigma_0}{\sigma_1 - \sigma_0} r_1 =$ $-\frac{t_2-t_0}{t_1-t_0}r_1$. Adding then an infinitesimal-sized circle to the "cusp", we get the trajectory $if(t < t_0, \sigma_1 + i.t_1 + r_1(cos(\alpha_1.t + \phi_1) - i.sin(\alpha_1.t + \phi_1)) + i.t_1 + i.t_2 + i.t_2 + i.t_3 + i.t_4 + i.t_4$ $\epsilon(\cos(\alpha_0.t + \phi_0) - i.\sin(\alpha_0.t + \phi_0)), \ \sigma_2 + i.t_2 + r_2(\cos(\alpha_2.t + \phi_2) - i.\sin(\alpha_2.t + \phi_0))$ $\phi_2)$) + $\epsilon(\cos(\alpha_0.t + \phi_0) - i.\sin(\alpha_0.t + \phi_0))$). Then a shift from $t = t_{00}$ to $t = t_{00} + dt$, dt > 0, means a shift of the trajectory sum by $\epsilon(\cos(\alpha_0)(t_{00} + t_{00}))$ dt) + ϕ_0) - $i.(sin(\alpha_0.(t_{00}+dt)+\phi_0)))$ which goes to the right and down as dtincreases, which either opens the cusp (for values ϕ_0 around $\phi_0 \approx -\alpha_0 t_{00}$) or is the starting point of a clockwise loop.

Each further increase of λ will provide the same situations leading to step j+1 completion when $\lambda=1$. This j to j+1 step can be repeated until a large enough j for which $\sum_{n=j+1}^{\infty}\frac{1}{n^s}$ will be negligible in front of $\sum_{n=2}^{j}\frac{1}{n^s}$ to have any annoyance on the local trajectory of the zeta function.





Proof. (2). A shorter proof is to assume the existence of a non-zero finite size counter-clockwise loop. In this case, recalling lemma 12 as σ increases, the corresponding trajectories are necessarily, at least partially (new loops may form), further and further outside that initial loop contradicting the fact that eventually the whole design must converges towards the point with coordinates (1,0).

Note. The figures 16B to 16E show the enlargement of a small loop while the last 16F displays a contraction. Of course, any intermediary figures may exist with same configuration result. A loop may also provide a smooth curve and a smooth curve may give a loop by some addition to a circle. What is of importance, as shown here, is that the cusp-like shape can be oriented in any direction vis-à-vis the circle and will still provides the required clockwise curvature. A counter-clockwise loop is impossible as it would need a repeated series of "aborted" loops with second parts in quite more outwards oriented left-direction trajectory than their first part inwards oriented right-direction trajectory. As the trajectories originate from circles and has thus locally balanced first and second part with it proper local almost axis of "symmetry", the inwards trajectory being always first, the process is "doundo" clockwise (but never "undo-do" clockwise). The additional clockwise benefit, due to the initial circles' clockwise shape, prohibit even the primer of a relevant counter-clockwise example.

Note. The k-th derivative of the Riemann Zeta function is defined over the complex plane Re(s) > 1 by

$$\zeta^{(k)}(s) = (-1)^k \sum_{n=1}^{\infty} \frac{(\ln(n))^k}{n^s}.$$

Let us focus on the transformation of this expression with increasing k whatever the value of the real part of s. We don't care here that this expression is no more the effective k-th derivative of the Riemann function and we do acknowledge that, within the critical band, we are outside the valid domain of definition but it doesn't really matter for our present purpose. In order to get the said derivatives, we add again circles but with the initial scaling factor $\ln^k(n)$ for each of them at the condition that we drop the sign given by $(-1)^k$. A positive scaling, that is a homothety, can't reverse a loop. As k increases, the trajectories are converging more and more towards circle-like loops turning around the origin with shapes approaching also that of the cases $\sigma << 0$, values of σ where the clockwise result is trivial. Therefore another hint in the same direction as the previous lemma.

Let us bring some additional developments to the previous note in regard to derivatives. Although, it may be partially in some vague form, it is nevertheless central to our investigation, as it contains critical arguments.

Lemma 15. The first derivative of the Riemann Zeta function implies the curves' shortening or elongation of the said function.

Proof. By definition, $\zeta(s+\epsilon) - \zeta(s) \to \zeta'(s)$. ϵ as $\epsilon \to 0$ and therefore the distances $\zeta(s+\epsilon) - \zeta(s)$ are locally shorter near the image's locus where $\zeta'(s)$ is small and are longer elsewhere. $\zeta'(s)$ is the direct and absolute gauge of the distances of the $\zeta(s)$ images.

Although one parameter is sufficient for our overview here, a more precise approach would be of course the use of the Jacobian matrix, the whole

linear transformations being formed by a rotation and a scaling. Tristan Needham, in his book "Visual Complex Analysis" calls these transformations amplitwists. [6]

This point generalizes of course to higher derivatives.

Lemma 16. The kinship lemma. The successive derivatives of the Riemann Zeta function have similar oriented designs modulo a sign adaptation.

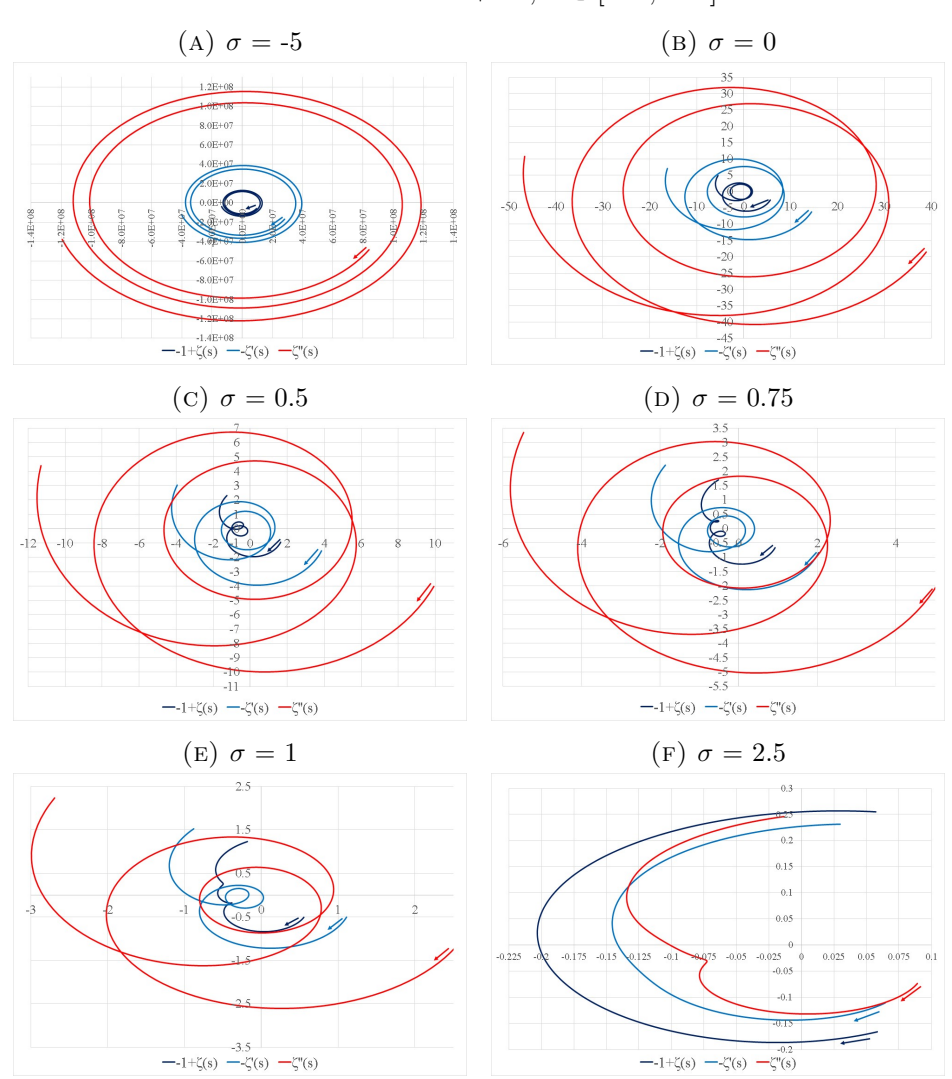
Proof. This is largely an immediate result of the previous lemma and is illustrated by the figures 17A to 17F. There is a feedback between the successive derived functions (downwards and upwards). As the reader may observe in the figures, for the 3 values of k chosen (k = 0, k = 1, k = 2), and this would hold for greater values, the trajectories have a lot of kinships, like starting and ending points on an approximative same line, general orientation, number of loops\aborted loops up to a certain stage, so long as we alternate the signs, therefore taking $-\zeta'$, $\zeta^{(2)}$, $-\zeta^{(3)}$, ..., when k increases and taking $-1+\zeta(s)$ instead of $\zeta(s)$ for the initial drawings. The kinship can be increase be using an adapted constant coefficient before each successive function. The need of alternate signs is therefore a mere observation for the said adapted constants' choices. Changes in rotations occurs and evolves in quite the same way as scalings do, that is progressively.

Lemma 17. Let us choose a horizontal line of ordinate t as the domain s and apply the Zeta function to it for $\sigma \in [0,1]$. As σ increases, the distance of the image $\zeta(s)$ to the coordinate (1,0) decreases systematically as soon as σ is greater than the abscissa of the closest zero z of the first derivative of the Zeta function.

Proof. In the absence of some peculiar opposite phenomena, $\zeta(s)$ is obliged to shrink exponentially towards (1,0) due to the parameter σ (for constant t). The only perturbative gauge is, according to lemma 15, the local field of first derivative's values. Thus, one can expect as soon as the distance to the position of a cancelling derivative starts to increase, the expression $\operatorname{norm}(\zeta(s)-1)$ must decrease exactly at that stage.

The figures 18A to 18D illustrate the previous lemma. Ahead of the said abscissa of the nearest first derivative's cancellation, on the contrary, one can observe in general an increase of the distance to (1,0). However, in that case, we still know that the trajectories of vertical lines are on the same side of each other. It is only after a loop described by $\zeta(s)$ has vanished that the image may take an adverse direction not heading further straight ahead as shown in the typical figures 12A to 12F. But, this is denied by the fact that, when a loop vanishes, it also means that the first derivative abscissa is just overcome and an irremediable road towards (1,0) is now set up. In the labels of the figures 18A to 18C, we indicate the coordinates z cancelling $\zeta'(z)$ and we chose the corresponding t values for the horizontal line's domains. In the figure 18D, the parameter t is taken off the ordinate

FIGURE 17. Kinship of $-1+\zeta$ and its sign-corrected derivatives. $s=\sigma+i.t,\,t\in[120,\,125].$



of the current zero of the first derivative. Therefore, the "potential well" due to the mentioned cancelling feature progressively disappears.

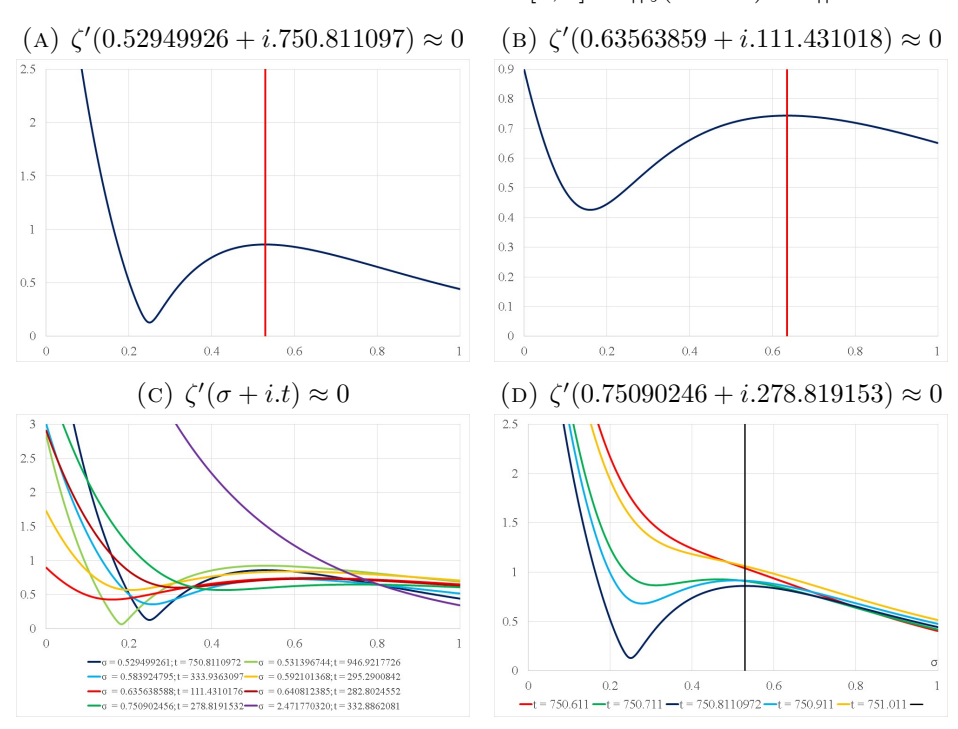


FIGURE 18. Evolution over $\sigma \in [0,1]$ of $||\zeta(\sigma+i.t)-1||_2$.

5.2.2. Adding oriented spirals.

Lemma 18. Let us consider a positive oriented vertical segment in the complex plane $s = \sigma + i.t$, $0 < \sigma \le 1$, $t \in [t_1, t_2]$, $t_1 >> 0$ and its image $\zeta(s)$. Then every loop in the image is only completed clockwise.

Proof. (1). According to theorem 3, for Re(s) > 0, the zeta function can be expressed as

$$\zeta(s) = \frac{s}{s-1} - s \int_1^\infty \frac{\{u\}}{u^{1+s}} du = \frac{s}{s-1} - s \sum_{n=1}^\infty \int_n^{n+1} \frac{\{u\}}{u^{1+s}} du.$$

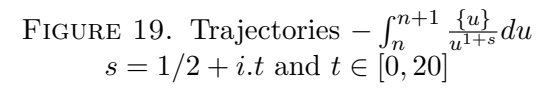
Because of the mantissa $\{u\}$, the expression $-\int_n^{n+1} \frac{\{u\}}{u^{1+s}} du$ describes, instead of a circle, an inwards clockwise spiral as illustrated by figure 19A for constant σ and increasing t. Locally, the clockwise bending will be therefore stronger than in the $\sigma > 1$ examples as the osculating circles possess smaller radius and therefore greater clockwise curvature in the second half of the cusp-like-shaped designs. The reverse loops are then even less implementable than previously and therefore inconceivable. Let us note that the effect of the mantissa diminishes very rapidly and even for small values of n, like n=10, the spirals converges already towards almost circles (see figure 19B). Let us note also that $\frac{1}{u^{1+\sigma}}$, $u \in [n, n+1]$, σ being some constant, has here again only a scaling effect with no changing effect on the general spiral

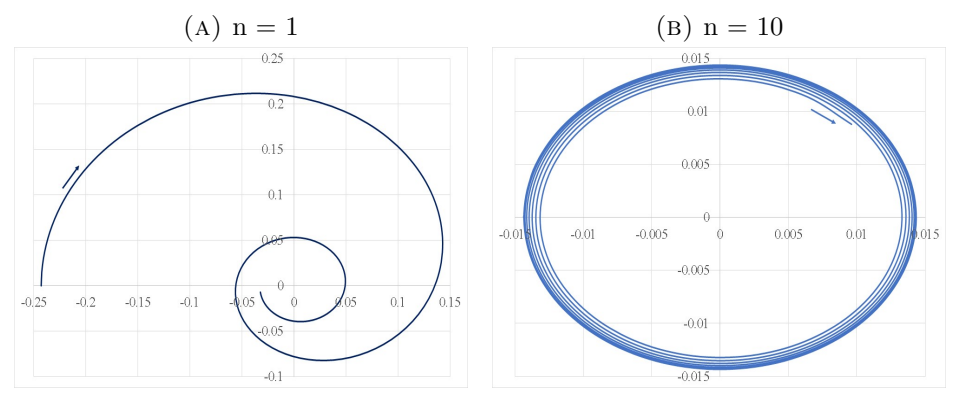
shape. Now, let us see the effect of the multiplier factor s on the integral when t >> 0. Locally, as a loop is forming, and the modulus of s is varying between $s_1 = \sigma + i.t_1$ and $s_2 = \sigma + i.t_2$, where t is in a range where a question remains on the existence of non-trivial zeros, the relative variation of s for the completion of the said loop is a factor quasi equal to 1. Therefore s is only a scaling factor on the loop with no effect on its intrinsic shape, less even so on some reversal. To finish with, the ratio $\frac{s}{s-1}$ tends towards 1 as t >> 0 and provides only a shifting of abscissa. Therefore the lemma.

Let us observe another way to get the same result. When we shift from $\sigma > 1$ to $0 < \sigma < 1$, the function $\zeta(s)$, and this is more so with greater values of t, is still well approximated by $\sum_{n=1}^{L} \frac{1}{n^s}$ when we choose some appropriate finite L instead of an infinite value. The reader is given the example of figure 20A and 20B. It is clear in these conditions that the prior circles additions' approach is still valid as again it is only a matter of a near factor 1 scaling.

Proof. (2). Refer word for word to proof 2 of lemma 14.
$$\Box$$

Let us note that the condition $t_1 >> 0$ in the lemma is not necessary as one can easily check the absence of counter-clockwise loops numerically for the contrary case.

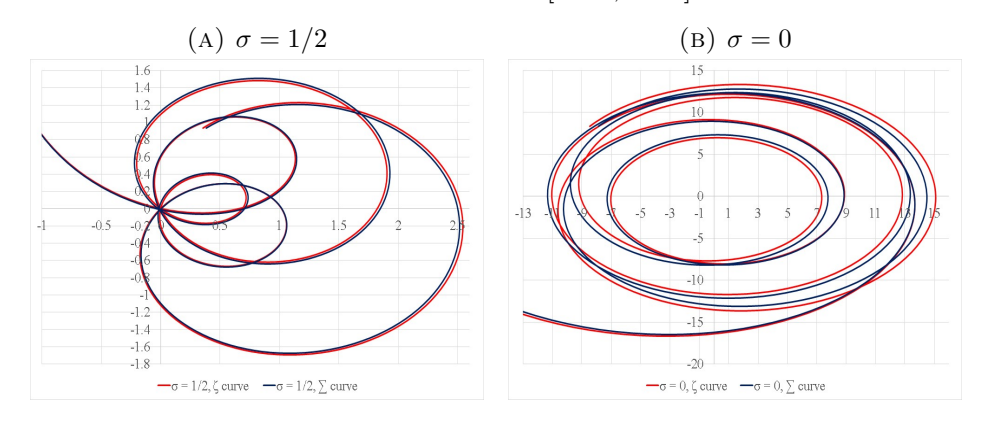




Note. For $\sigma < 0.5$, numerical checks display no counter-clockwise piece of trajectory of the Riemann zeta function's image whatsoever. For $\sigma \geq 0.5$, numerical checks provide only counter-clockwise pieces of trajectory deviations of the tangent vectors adding up to a total value of π radians at most preventing as said the primer example of a counter-clock loop.

5.3. The simplified context. The "complexity" of the graphics' designs are due entirely to the zeros of the derivatives of the Zeta function. It is possible however to simplify greatly the drawings by using another function.

FIGURE 20. Trajectories $\zeta(s)$ and approximation $\sum_{n=1}^{500} \frac{1}{n^s}$ $s = \sigma + i.t$ and $t \in [1000, 1006]$



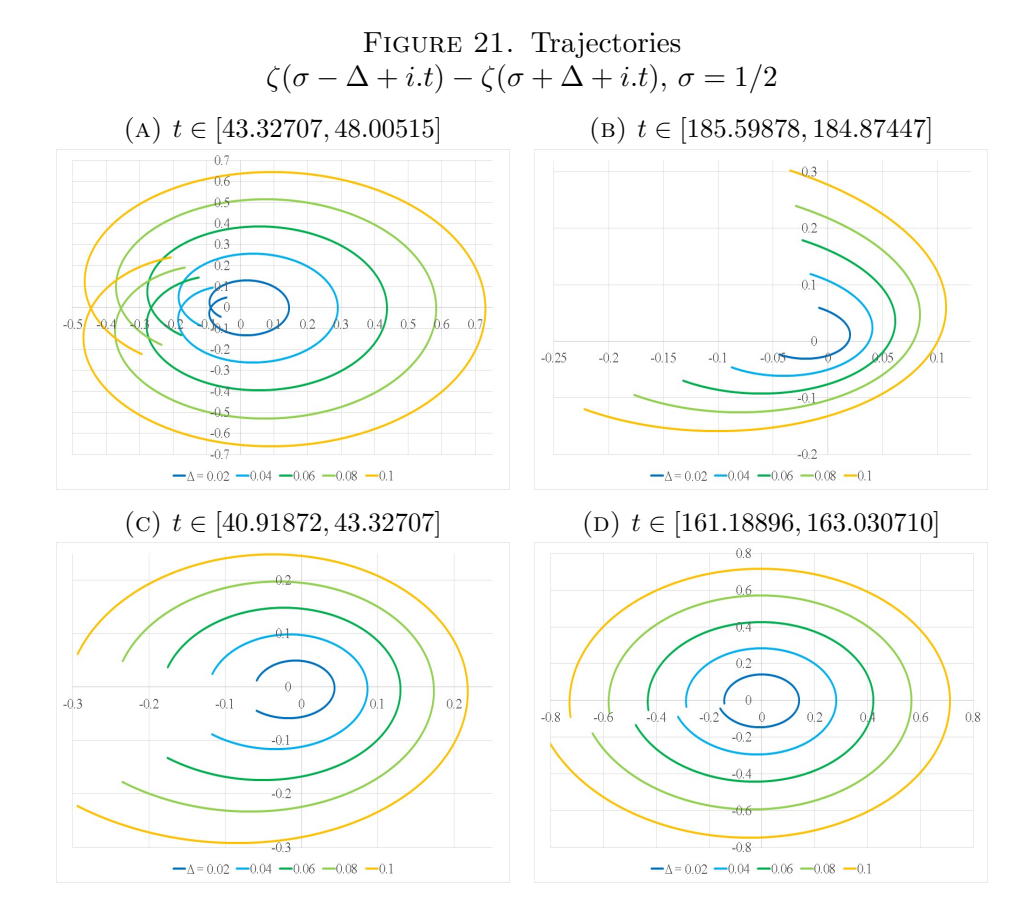
Indeed, trying to solve $\zeta(1/2 - \Delta + i.t) = \zeta(1/2 + \Delta + i.t) = 0$, we may rather start by solving $\chi(\Delta,t) = \zeta(1/2 - \Delta + i.t) - \zeta(1/2 + \Delta + i.t) = 0$ and then $\zeta(1/2 + \Delta + i.t) = 0$ for example. This leads us to study $\chi(\Delta,t)$ in a general way. The figures 21A to 21D are the "cousins" of the figures 11 and 12 as we step from the ζ -function to the χ -function. These figures keep similitudes as long as the zeros of the derivative are not reached (in the initial figures), in particular for the extent of the rotations around their respective "centres". But no first derivative cancellations to be considered any more at least apparently. Each of the graphs seems to be almost homothetic in regard to the coordinate (0,0) and therefore the only solution to $\chi(\Delta,t)=0$ would be $\Delta=0$. The questions are then "can we trust the obvious?" and "where are now the zeros of the derivative hiding?".

5.4. A mix graphic-analytic proof. Without divulging prematurely the answers to the two previous questions, let us say that we need to deviate from our so far choice $\sigma = 1/2$. Let us have a more general approach by writing $\chi(\sigma, \Delta, t) = \zeta(\sigma - \Delta + i.t) - \zeta(\sigma + \Delta + i.t)$ and let us choose $0 \le \Delta \le 1/2$ and t > 0.

Lemma 19. The function $\chi(\sigma, \Delta, t)$ is an odd function in regard to the variable Δ .

$$\begin{array}{l} \textit{Proof.} \ \chi(\sigma, -\Delta, t) = \zeta(\sigma + \Delta + i.t) - \zeta(\sigma - \Delta + i.t) = -(\zeta(\sigma - \Delta + i.t) - \zeta(\sigma + \Delta + i.t)) = -\chi(\sigma, \Delta, t). \end{array}$$

Note. This means that the function $\chi(\sigma, \Delta, t)$ is symmetrical in regard to (0,0). If one is interested to the solutions of $\chi(\sigma, \Delta, t) = 0$, it is therefore necessary and sufficient to study the function on the half line $\Delta \geq 0$. Let us note then that $\Delta = 0$ is an obvious solution to $\chi(\sigma, \Delta, t) = 0$ and if it is the only solution for arbitrary σ , it will be for $\sigma = 1/2$ meaning we are done with the Riemann hypothesis.



Definition 3. Let us consider a closed circular neighbourhood of $s = \sigma + i.t$, not reduced to a point, in the complex plane and $[\sigma_{min}, \sigma_{max}]$ the range of values of the abscissas over that neighbourhood, $\sigma_{min} \leq \sigma \leq \sigma_{max}$. The function $\chi(\sigma, \Delta, t)$ is said to be locally well-ordered over the previous neighbourhood of s if its trajectories are strictly on the same side to each other as Δ strictly increases over the whole range $[\sigma_{min} - \sigma, \sigma_{max} - \sigma]$, σ and t is being kept constant. One may alternatively say that the trajectories are well-ordered (instead of the function).

Lemma 20. The function $\chi(\sigma, \Delta, t)$, t > 0, is locally well-ordered for small enough Δ except at the zeros of the derivative of the Zeta function. Moreover, it is a local approximate homothety in regard to Δ .

Proof. Note first that the condition $t \neq 0$ secludes the Zeta function pole. We can write then the Taylor series:

$$\chi(\sigma, \Delta, t) = -2 \sum_{n=0}^{n=+\infty} \frac{\Delta^{2n+1}}{(2n+1)!} \zeta^{(2n+1)}(\sigma + i.t).$$

Now, for some multiplicative factor r and using $s = \sigma + i.t$, we get

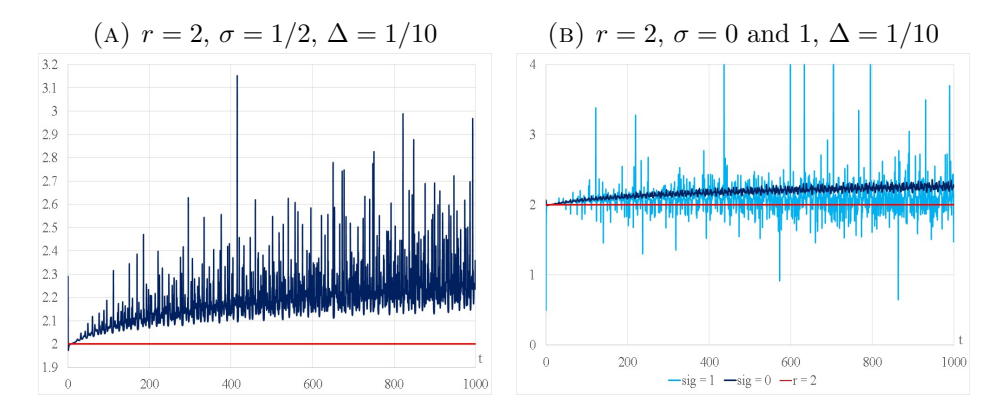
$$\rho(r,\sigma,\Delta,t) = \frac{\chi(\sigma,r.\Delta,t)}{\chi(\sigma,\Delta,t)} = r \frac{\zeta'(s) + r^2 \frac{\Delta^2}{6} \zeta^{(3)}(s) + r^4 \frac{\Delta^4}{120} \zeta^{(5)}(s) + \cdots}{\zeta'(s) + \frac{\Delta^2}{6} \zeta^{(3)}(s) + \frac{\Delta^4}{120} \zeta^{(5)}(s) + \cdots}.$$

Whatever the finite given values of σ and Δ , $\chi(\sigma, r.\Delta, t)$ is finite (being off the pole of the Zeta function). For small enough values of Δ and supposing $\zeta'(s) \neq 0$, $\rho(r, \sigma, \Delta, t) \approx r$, hence the local approximate homothety (which means also that the function is well-ordered).

The homothety is of course approximative. As Δ is given larger values, and the first terms in the numerator and denominator are no more the leading ones, the most likely to become so are then the second terms of the fraction, thus $\rho(r,\sigma,\Delta,t)$ will tend towards r^3 . One therefore would expect, taking this time a fixed moderate value of Δ and varying instead t, to get for $\rho(r,\sigma,\Delta,t)$ values between r and r^3 , mostly near but superior to r and experiencing in general peaks of height smaller than r^3 . Figure 22A gives an illustration of such evolution of $\rho(r,\sigma,\Delta,t)$ choosing $\sigma=1/2$ and $\Delta=1/10$. Except close to the origin, we see the systematic values over the chosen homothety threshold r=2 and the narrow peaks.

One can of course envision to have the first and second terms negligible providing even higher ratios. Such occurrences are obviously exceptional. Now, checking the evolution of $\rho(r,\sigma,\Delta,t)$ in regard to σ , let us signal figure 22B in addition to figure 22A. For moderate Δ , on the left hand side of the critical line, the expression does not vary much. It oscillates mildly above the ratio r. Heading towards the right hand side of the critical line instead, the ratio will start to show counterexamples to the interval $[r, r^3]$, notably with values smaller than r. Indeed near a zero of the derivative, with an arbitrary choice of Δ , one cannot guess in advance which of the numerator or denominator will be larger in $\frac{\rho(r,\sigma,\Delta,t)}{r}$. However, the reader can always choose a smaller value of Δ to re-establish the local homothety.

FIGURE 22. Evolution of $||\rho(r, \sigma, \Delta, t)||_2$



Lemma 21. A solution s to $\zeta(s + \Delta) = 0$ and $\chi(\sigma, \Delta, t) = 0$ is necessarily a double zero of the Zeta function.

Proof. If $\zeta'(s) = 0$,

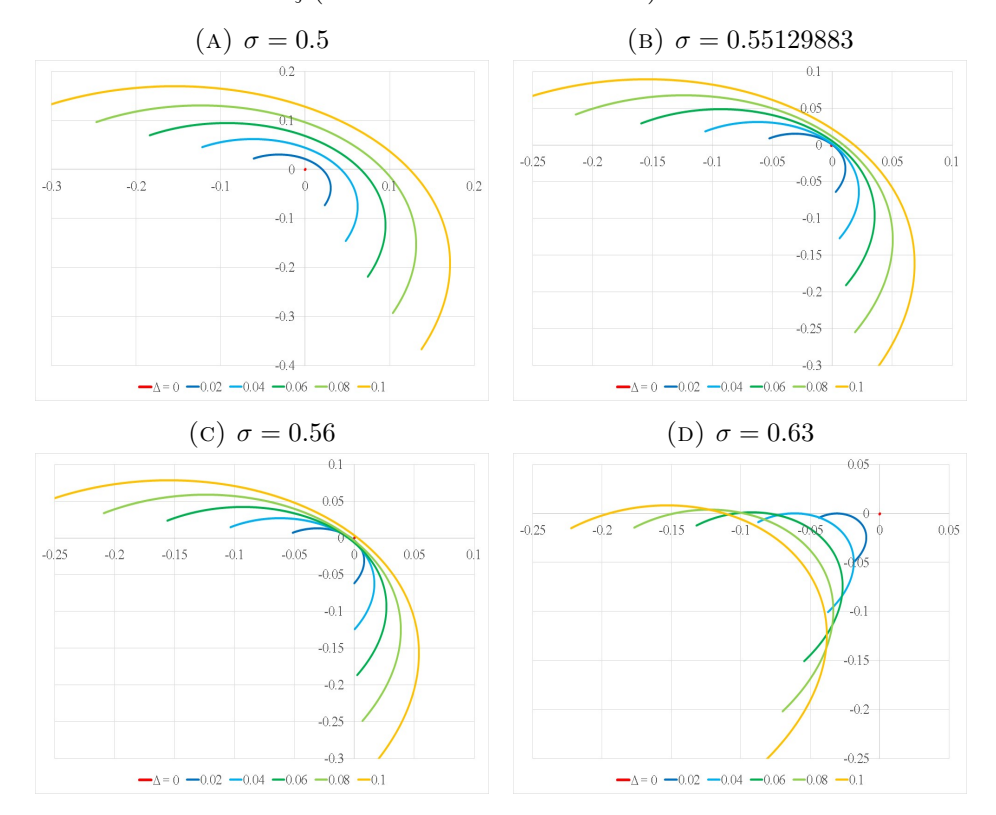
$$\chi(\sigma, \Delta, t) = -2 \sum_{n=1}^{n=+\infty} \frac{\Delta^{2n+1}}{(2n+1)!} \zeta^{(2n+1)}(s)$$

and thus

$$\rho(r,\sigma,\Delta,t) = r^3 \frac{\frac{\Delta^2}{6} \zeta^{(3)}(s) + r^2 \frac{\Delta^4}{120} \zeta^{(5)}(s) + \cdots}{\frac{\Delta^2}{6} \zeta^{(3)}(s) + \frac{\Delta^4}{120} \zeta^{(5)}(s) + \cdots} \to r^3.$$

We may have simplified the fraction by $\frac{\Delta^2}{6}$ but we left it here on purpose to show that, as Δ tends towards 0, numerator and denominator tend also towards 0, that is $\chi(\sigma, \Delta, t) \to 0$. The figures 23A to 23C illustrate in a concrete way what happens in the case where we choose a sample of small enough fixed values of Δ and some interval $[t_1, t_2]$ and we shift progressively the parameter σ from an abscissa on the left side of a zero of the derivative of the Zeta function up to the abscissa of the said zero and then beyond that same zero. Here we chose the starting abscissa $\sigma = 0.5$ as we picked for our illustration the 168th zero of the derivative characterized by its relative proximity to the critical line. The following arguments would be the same if we had to face a zero of the derivative with abscissa lower than 1/2 as the knowledge of its effective value is not needed to proceed. The first picture, figure 23A, shows the almost homothetic pattern over the whole range $[t_1, t_2]$. In the absence of a particular event, the crossing of the center (0,0) cannot start except if $\Delta = 0$. The second picture, figure 23B, which is brought with a closer view, shows, because of the evolution towards the degree 3 of r, an accelerated narrowing of the curves near the position corresponding to the zero of the derivative. Still being an almost local homothety (but with larger local ratio near the image coordinate (0,0), no crossover of the curves can occur on this stage. That crossover can and will only occur as σ takes values beyond the derivative's zero abscissa (see figure 23C). Note before going further that this is in no way contradictory to the same sides' pattern cited for the Zeta function context. Effectively, the function $\chi(\sigma, \Delta, t)$ is analytic (away from the pole of the Zeta function), but the conformal map property does not apply here because we cannot write the function as an expression of only one variable s (the reader may refer to the note made next to theorem 2), but we need instead two of them s and Δ in $\chi(s,\Delta) =$ $\zeta(s-\Delta)-\zeta(s+\Delta)$. Back to the main subject, we get the start of the crossing of the coordinate (0,0) and the failure of the well-ordered trajectories by $\chi(\sigma, \Delta, t)$ at the precise place where simultaneously $\zeta'(s) = 0$ and Δ is taking its limit value 0. This is equivalent to say that $\zeta'(s+\Delta)=0$ at that peculiar event. Now, seeking to solve the additional event $\zeta(s+\Delta)=0$, this means that the latest zero is necessarily a double zero. If $\chi(\sigma, \Delta, t) = 0$, the events $\zeta(s+\Delta)=0, \zeta'(s+\Delta)=0$ are simultaneous events, hence the lemma.

FIGURE 23. Trajectories $\chi(\sigma, \Delta, t)$, $t \in [415.018810, 415.455215]$, $\zeta'(0.55129883 + 415.247512i) \approx 0$



Note. If some event doesn't exist at all, one can only simulate what would happen if the said event would occur. Obviously it is impossible to display it, hence $\Delta \to 0$ necessarily in our presentation when passing to the limit.

Note. In the previous argument, we mentioned the evolution of figures 23A to 23C with increasing σ . However, we didn't prove that this evolution is necessarily in that direction. We may have instead that order of drawings' patterns with decreasing σ . Indeed, in the vicinity s where $\zeta'(s) \to 0$, and with $r \approx 1$, we recall to have

$$\rho(r, \sigma, \Delta, t) = r \frac{\zeta'(s) + r^2 \frac{\Delta^2}{6} \zeta^{(3)}(s) + \cdots}{\zeta'(s) + \frac{\Delta^2}{6} \zeta^{(3)}(s) + \cdots}.$$

The local homothety ratio's progressive evolution between r and r^3 is only true on one side of the σ_0 value such that $\zeta'(s_0) = 0$, this side being either on the left or on the right of σ_0 according to the local sign of the ratio $\zeta^{(2k+1)}(s)/\zeta'(s)$ where k is the smallest natural number such that $\zeta^{(2k+1)}(s_0) \neq 0$. Indeed this is the result of the following calculation, where

we use $(1+\epsilon_1)/(1+\epsilon_2) \approx 1+\epsilon_1-\epsilon_2$ to evaluate the former ratio (at $s \neq s_0$ and small enough Δ),

$$\begin{array}{ll} \rho(r,\sigma,\Delta,t) &\approx & r\cdot(1+(r^2-1)\frac{\Delta^{2k}}{2k+1}\frac{\zeta^{(2k+1)}(s)}{\zeta'(s)})\\ &\approx & r\cdot(1+(r^2-1)\frac{\Delta^{2k}}{2k+1}(\Re(\frac{\zeta^{(2k+1)}(s)}{\zeta'(s)})+i.\Im(\frac{\zeta^{(2k+1)}(s)}{\zeta'(s)})))\\ \text{where }\Re(c)\text{ et }\Im(c)\text{ are respectively the real and imaginary parts of some} \end{array}$$

complex number c.

Hence, using $\Delta^{2k} >> \Delta^{4k}$ ($|\Delta| << 1$) in the second equality underneath and $(1+2\epsilon)^{1/2} \approx 1+\epsilon$ in the third one,

$$||\rho(r,\sigma,\Delta,t)||_{2} \approx r \cdot \{(1+(r^{2}-1)\frac{\Delta^{2k}}{2k+1}\Re(\frac{\zeta^{(2k+1)}(s)}{\zeta'(s)}))^{2} + ((r^{2}-1)\frac{\Delta^{2k}}{2k+1}\Im(\frac{\zeta^{(2k+1)}(s)}{\zeta'(s)}))^{2}\}^{\frac{1}{2}}$$

$$\approx r \cdot \sqrt{1+2(r^{2}-1)\frac{\Delta^{2k}}{2k+1}\Re(\frac{\zeta^{(2k+1)}(s)}{\zeta'(s)})}$$

$$\approx r \cdot (1+(r^{2}-1)\frac{\Delta^{2k}}{2k+1}\Re(\frac{\zeta^{(2k+1)}(s)}{\zeta'(s)}))$$

It happens that the left case (that is here $\Delta > 0$) seems to be always the wellordered side. It is at least so for the sample up to $0 < t \le 1000$ for which we chose to draw the figures 24A and 24B. The ratio $\frac{\zeta^{(3)}(s)}{\zeta'(s)}$ is not only always positive but usually greater than $1/\Delta$. In the studied interval, and with the choice $\Delta = 1/1000$, only 1 in 100 are lower than the resulting "1000" threshold. Note also that $\zeta^{(3)}(s_0)$ is very likely different from 0, and therefore the usually adapted value of k is 1 (hence we can rely on the ratio $\frac{\zeta^{(3)}(s)}{\zeta'(s)}$ to conduct the calculation of a sample). In order to prove the systematic left hand side conjecture, one would need for example a precise Weierstrass factorisation of $\zeta'(s)$, which would allow to get the exact expression of the ratio $\frac{\zeta^{(2)}(s)}{\zeta'(s)}$ and then of $\frac{\zeta^{(3)}(s)}{\zeta'(s)} = (\frac{\zeta^{(2)}(s)}{\zeta'(s)})' + (\frac{\zeta^{(2)}(s)}{\zeta'(s)})^2$. Of course, as σ increase further on the right side of the abscissa of the

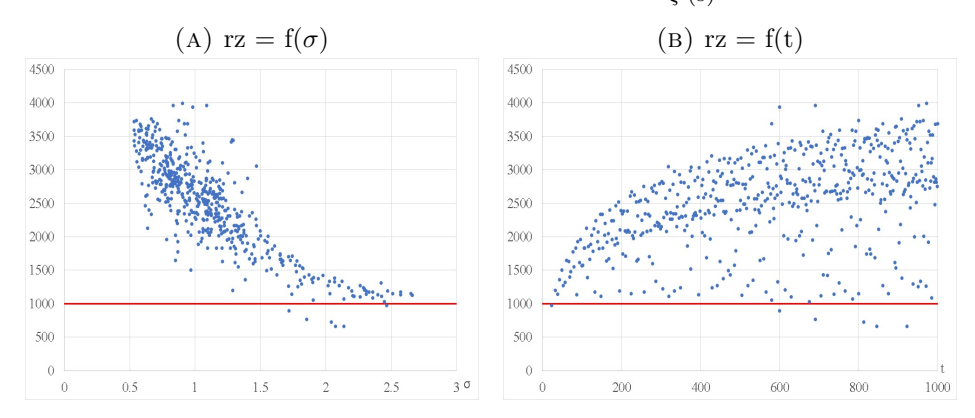
zero of the derivative, where the homothety fails, there will be nevertheless usually a progressive return to the near homothety of ratio r as shown in figure 23D.

Theorem 9. The Riemann hypothesis is true.

Proof. Theorem 6 and lemma 21 are incompatible. Therefore it is impossible to have $\zeta(s+\Delta)=0$ and $\chi(\sigma,\Delta,t)=0$ simultaneously if $\Delta\neq 0$, therefore $\zeta(s+\Delta)=0$ and $\zeta(s-\Delta)=\chi(\sigma,\Delta,t)+\zeta(s+\Delta)=0$ in the same time. Theorem 5 allows us then to conclude.

Note. To be very precise, following the proof in lemma 21 and the note that follows it, our full argumentation is not immediately equivalent to say that $\zeta(s+\Delta)=0$ and $\zeta(s-\Delta)=0$ is impossible if $\Delta\neq 0$, but it proves that $\zeta(s+\Delta)=0$ and $\zeta(s-\Delta)=0$ if and only if $\Delta=0$ which is definitely the same.

FIGURE 24. Evaluation $rz = \Re(\frac{\zeta^{(3)}(s)}{\zeta'(s)})$



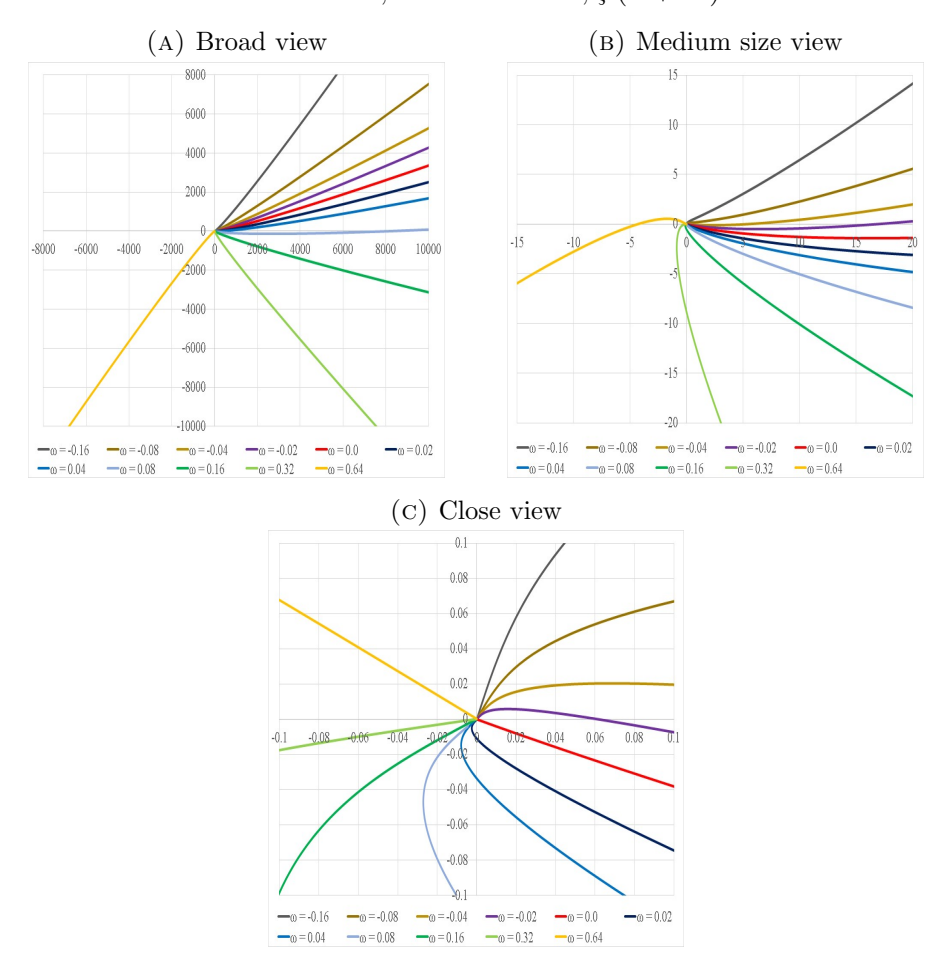
Another approach is to consider some initial fixed σ and t values and varying the parameter Δ . We get that way orthogonal trajectories to the previous ones. We give then different evolving values to t, this parameter becoming progressively $t+\omega$. Let start our drawing at some zero of the Zeta function derivative as illustrated by the figures 25A to 25C, which represent the same trajectories but at various axes' scales. At that zero of the said derivative of Zeta, the function $\chi(\sigma, \Delta, t)$ is given by the following lines of equalities

$$\begin{array}{ll} \chi(\sigma,\Delta,t) &= \zeta(\sigma-\Delta+i.t) - \zeta(\sigma+\Delta+i.t) \\ &= \zeta'(\sigma+i.t)(-\Delta) + \zeta''(\sigma+i.t)(\Delta^2) + \text{higher orders terms} \\ &= \zeta''(\sigma+i.t)(\Delta^2) + \text{higher orders terms}. \end{array}$$

Because the leading term has a factor Δ^2 , the trajectory is a straight line outwards and does not allow for a self-crossing of the trajectory near that initial point (where $\Delta=0$). Choosing an initial trajectory, then only evolving continuously one parameter (the parameter t towards $t+\omega$), the sum of two analytic functions being an analytic function, the trajectories do not cross each other locally, therefore forming a star plot, unless a zero of the derivative of $\chi(\sigma, \Delta, t+\omega)$ is encountered along their spiralling path. In the later case, one knot (self-crossing) would form and grow in size with increasing ω (in order not to cross itself), which is absurd as it would mean that $\zeta(\sigma - \Delta + i.t) = \zeta(\sigma + \Delta + i.t)$ for some huge values of Δ .

Note. Instead of varying t only (with the addition of the value ω) as we did in the figure 25, we may choose rather to vary the position of the initial end point (at $\Delta=0$) by moving to another final point using a straight line in the complex plane domain (that is σ and ω are evolving together). We get the exact same type of trajectories as illustrated by the figures 26. This is a strategy, one can choose to "link" any final point on the critical line as the "result" of the choice of an initial point equal to a zero of the derivative of the Zeta function. One, of course, would choose the closest zero (of the

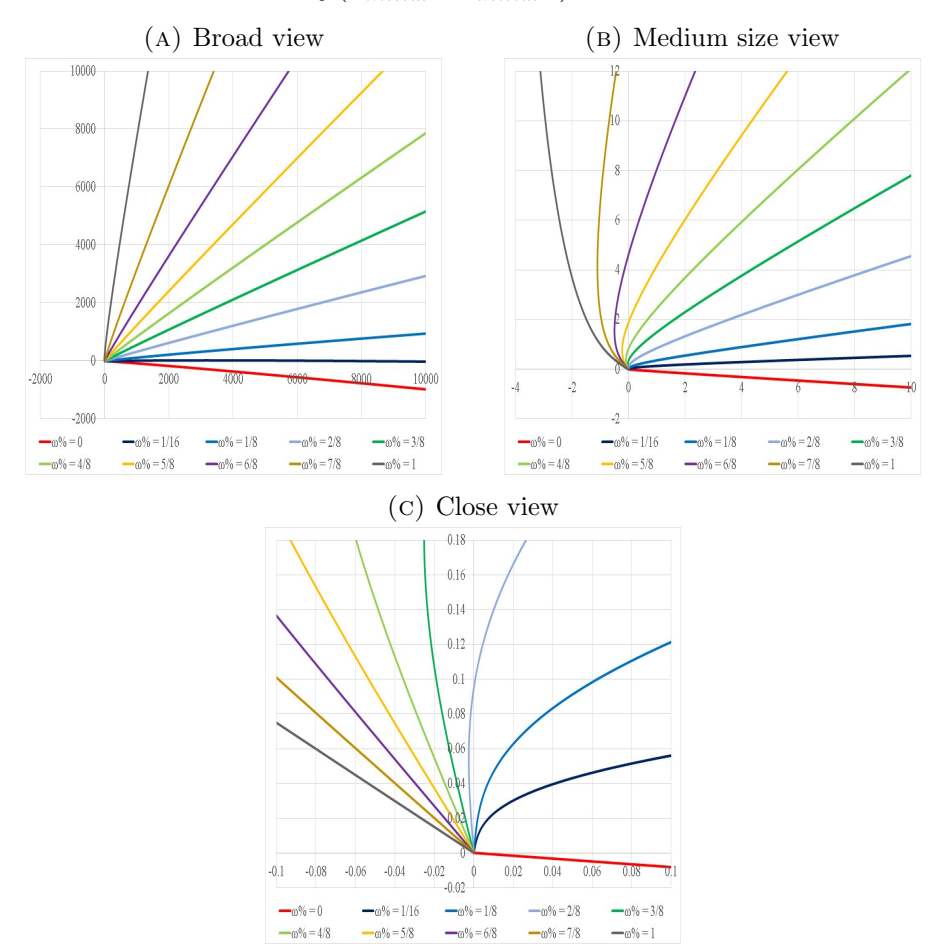
FIGURE 25. Trajectories $\chi(\sigma, \Delta, t + \omega)$, $\Delta \in [0, 1]$, $\sigma \approx 0.994353167, t \approx 324.468750, <math>\zeta'(\sigma + t.i) \approx 0$.



derivative of the Zeta function) to built the "experiment", but any other may suit likewise. Moreover, one doesn't have to start with a zero (of the derivative) but at any point of the complex plane where one observes no knot on the trajectory (when Δ increases from 0 to ∞ . It is easy to find one such initial point anywhere in the complex plane, it means that $\chi(\sigma, \Delta, t) = 0$ is impossible whatever the initial choice of σ and t when Δ increases from 0 to ∞ . Note also that instead a straight line in the domain we can also choose any smooth path). Therefore again confirming the Riemann hypothesis.

Note. One may object the property of no self-crossing at the view of the contrary when changing only one thing in the previous "experiment" that is instead of having Δ taking increasing real values, it is given imaginary values as in figure 27. Observe that in this case the crossing occurs because,

FIGURE 26. Trajectories $\chi(\sigma, \Delta, t)$, $\sigma_{initial} \approx 0.53428928$, $t_{initial} \approx 564.3344206$, $\sigma_{final} \approx 0.5$, $t_{final} \approx 564$, $\zeta'(\sigma_{initial} + t_{initial}.i) \approx 0$.

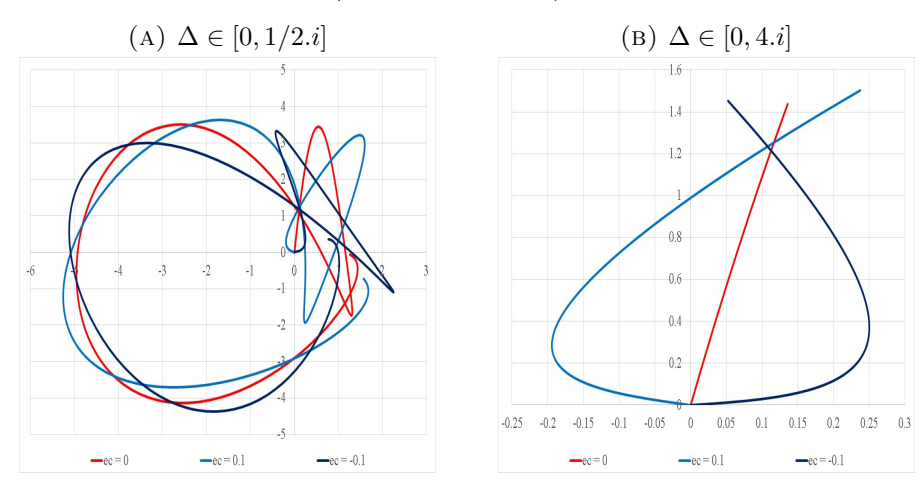


one cannot build an initial curve without self-crossing and therefore the curves will alternate sides one to the other, even if we still have an analytic function where we choose a unique parameter, the change in directions of the trajectory corresponding to nearby zeros of the derivative of $\chi(\sigma, \Delta, t_{initial} + \omega)$ relative to this parameter (here precisely ω). Note also that even in this case, one needs to get higher values for Δ than 1/2.i to get a crossover.

6. An alternative graphical context and proof

Let us consider the trajectories of the function $\varpi(s) = -\frac{\zeta(s)}{\zeta'(s)}$, $s = \sigma + i.t$ for different given values of σ within the critical upper band (t > 0). Let us examine first the case $\sigma = 1/2$ as shown in the figures 28A and 28B. After

FIGURE 27. Trajectories $\chi(\sigma, \Delta, t + ec)$, $\sigma_{initial} \approx 0.53428928$, $t_{initial} \approx 564.3344206$, $\zeta'(\sigma_{initial} + t_{initial}.i) \approx 0$.



an initial catch-up with the first zero of the Zeta function, the trajectory is trending towards circle-like paths with diminishing radii. As shown in the figure with index B, the almost circular paths are already reached as soon as the ordinate t=100, the trajectories C_i being those of the studied curves and C_i' being those of the curves $r(1+\cos(2\pi(t-\frac{1}{2}))+i.\sin(2\pi(t-\frac{1}{2})))$. It shows therefore a much more regular picture than the traditional analogous trajectories delivered by the Zeta function with its constant return to the coordinate (0,0) when $\sigma=1/2$ but various erratic in-between distances to that locus (remember figure 1). Such novel regularity speaks by itself in favour of the Riemann hypothesis.

Let us however go in deeper considerations, first by pointing at the origin of the almost circular shapes.

Theorem 10. The ratio of the Zeta derivative to the Zeta function is provided by the exact formula

$$\frac{\zeta'(s)}{\zeta(s)} = \ln 2\pi - \frac{1}{2}\gamma - 1 - \frac{1}{s-1} - \frac{1}{2}\frac{\Gamma'(\frac{1}{2}s+1)}{\Gamma(\frac{1}{2}s+1)} + \sum_{\rho} (\frac{1}{s-\rho} + \frac{1}{\rho})$$

where Γ is the well-known gamma function, $\gamma = -\frac{\Gamma'(1)}{\Gamma(1)}$ is the Euler-Mascheroni constant and ρ are the non-trivial zeros of the Zeta function.

Proof. This theorem is an immediate result of the Hadamard product for the Zeta function [11]. \Box

As t increases, $\frac{1}{s-1}$ tends towards 0, while $\frac{\Gamma'(\frac{1}{2}(\sigma+i.t)+1)}{\Gamma(\frac{1}{2}(\sigma+i.t)+1)} - \frac{\Gamma'(\frac{1}{2}(\sigma+t)+1)}{\Gamma(\frac{1}{2}(\sigma+t)+1)}$, where we substitute willfully the imaginary ordinate i.t with the real value t, is heading towards $\frac{\pi}{2}i - (1+i)\frac{1+\sigma}{t}$ as numerical checks indicate easily. Now,

for a natural number n, the Digamma function $\psi(n) = \frac{\Gamma'(n)}{\Gamma(n)}$, according to reference [12], is equal to $\psi(1) + H_{n-1}$ where H is the harmonic function $(H_n = \sum_{1}^{n} \frac{1}{n})$, so that for large enough t, we get

$$\frac{\Gamma'(\frac{1}{2}s+1)}{\Gamma(\frac{1}{2}s+1)} \approx \frac{\pi}{2}i - (1+i)\frac{1+\sigma}{t} + \psi(1) + H_{\lfloor (t+\sigma)/2 \rfloor}
= \frac{\pi}{2}i + \psi(1) + H_{\lfloor (t+\sigma)/2 \rfloor} + o(\frac{1}{t}).$$

Therefore, for t >> 100,

$$\frac{\zeta'(s)}{\zeta(s)} = \ln 2\pi - 1 - \frac{1}{2}H_{\lfloor (t+\sigma)/2 \rfloor} - \frac{\pi}{4}i + \sum_{\rho} (\frac{1}{s-\rho} + \frac{1}{\rho}) + o(\frac{1}{t})$$

This shows that there is no diverging contribution to $\frac{\zeta'(s)}{\zeta(s)}$ when s tends towards ρ except the term $\frac{1}{s-\rho}$. Hence, when s tends towards ρ^- from beneath values of t, $\frac{\zeta'(s)}{\zeta(s)}$ will diverge towards $-i.\infty$ and when s tends towards ρ^+ from above, $\frac{\zeta'(s)}{\zeta(s)}$ will diverge towards $+i.\infty$ in a systematic way. Some zero ρ_i and its successor ρ_{i+1} are extremely narrow values compared to ∞ and therefore $\frac{\zeta'}{\zeta}(s)$, in that interval, is analogous to an almost vertical line in the complex plane. Then, let us introduce the following lemma.

Lemma 22. The multiplicative inverse of a vertical line in the complex plane is a circle.

Proof. Let us consider the line 1+i. $\tan(u)$ where $u \in]-\frac{\pi}{2}, \frac{\pi}{2}[$ and which is the vertical line passing through (1,0) which trajectory is described exactly one time as the interval $]-\infty.i,\infty.i[$.

Then
$$\frac{1}{1+i.\tan(u)} = \frac{1-i.\tan(u)}{1+(\tan(u))^2} = \cos^2(u)(1-i.\tan(u)) = \cos^2(u)-i.\sin(u)\cos(u)$$

= $\frac{2\cos^2(u)-i.2\sin(u)\cos(u)}{2} = \frac{\cos^2(u)+1-\sin^2(u)-i.2\sin(u)\cos(u)}{2} = \frac{(1+\cos(2u)+i.\sin(2u))}{2}$

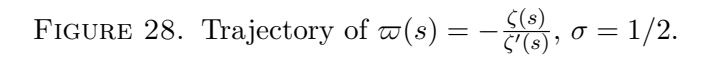
which is the circle of center (1/2,0) and diameter 1/2 in the complex plane. Its trajectory is described exactly one time except the point (0,0) which may be included by continuity.

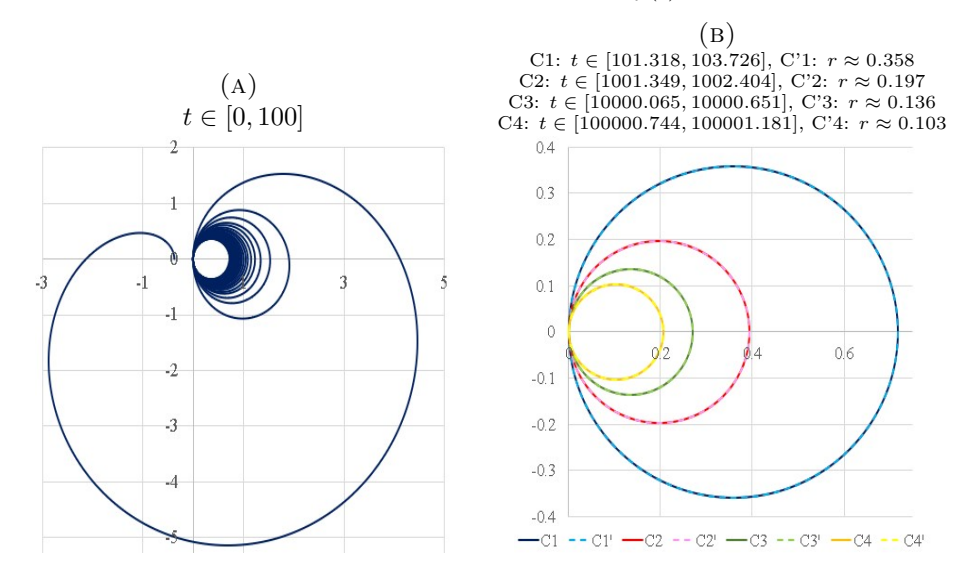
Therefore the reciprocal of the vertical line $\frac{2}{r}(1+i.\tan(\pi(t-\frac{1}{2})))$, where r is some strictly positive real number and $t \in [0,1[$, is precisely the circle $r(1+\cos(2\pi(t-\frac{1}{2}))+i.\sin(2\pi(t-\frac{1}{2})))$.

Here, while r decreases, the vertical lines are shifted to the right and their reciprocal inverses are circles inside each other with common coordinate (0,0) and centre on the real axis.

The corresponding opposite multiplicative inverse $-\frac{\zeta}{\zeta'}(s)$ of the previous ratio $\frac{\zeta'(s)}{\zeta(s)}$ will therefore exhibit, according to lemma 22, between two zeros, more accurate circular trajectory as t is given progressively higher values.

Moreover, the initial vertical lines shift always in the same direction (increasing t) and therefore the circles i + 1 are systematically inscribed in the circles i (with common coordinate (0,0)).





Lemma 23. The function $\varpi(s)$ trajectory in the complex plane, for $\sigma = 1/2$ and t > 0 is composed of inscribed circles, with common coordinate (0,0), if and only if there are no zeros of $\zeta'(s)$ on the critical line.

Proof. This is an immediate result from the ending argument at the previous section as we can reverse obviously the initial equation $\frac{\zeta'(s)}{\zeta(s)}$ if and only if $\zeta'(s) \neq 0$.

We have proven that there are no double zeros of the Zeta function. Therefore the remaining problematic cases s, focusing only on the critical line, are isolate coordinates 1/2 + i.t such that $\zeta(1/2 + i.t) \neq 0$ and $\zeta'(1/2 + i.t) = 0$.

Lemma 24. The function $\varpi(s)$ trajectories in the complex plane, for $\sigma < 1/2$ and t > 0, remain on the same side one to each other as σ decreases to abscissa 0.

Proof. The function $\varpi(s)$, as the ratio of two analytic functions, is analytic everywhere except where its denominator, here $\zeta'(s)$, cancels. The function is therefore a local bijection, according to theorem 2, that is with no-crossing trajectories. A single numerical check will tell the side where all the other respective oriented trajectories will be located. Where $\zeta'(s)$ cancels, is the place where the curves get the closest to each other without touching however

(as zeros of none constant analytic functions are isolated in any reference frame). $\hfill\Box$

The figures 30A to 30B illustrate the trajectories of $\varpi(s)$ for different pieces of vertical lines t which are ordinates between two zeros of $\zeta(s)$. We chose equidistant segments on the domain critical band and some additional abscissa when relevant. We get again two types of configurations (as it was the case in figures 11 and 12), linked to the same reason that is, the cancellation or not of the derivative (here $\varpi'(s)$). But there is often an additional type of event which corresponds to the case where $\zeta'(s) = 0$ leading then to the divergence of $\varpi(s)$. Unlike that picture in figure 12D in which the evolution with increasing σ may seem to have a chance in some other even "luckier" instance to return to (0,0) (which is not the case as the actual attractor is the coordinate (1,0)), here the successive paths will head towards always smaller inner designs heading to the center of the "initial" circle (the one for $\sigma = 1/2$) and distancing irremediably away from the original coordinate (0,0).

Let us note also that the presence of a derivative in the section is not detrimental to the argument as it has the effect to shorten faster the length of the pieces of trajectories. In addition to that remark, it is pertinent also to note the effect of larger t in a faster shrinking of the trajectories with equal increase of σ , remembering here that there has being established the absence of non-trivial zeros outside the critical line at least up to $t \approx 10^{20}$.

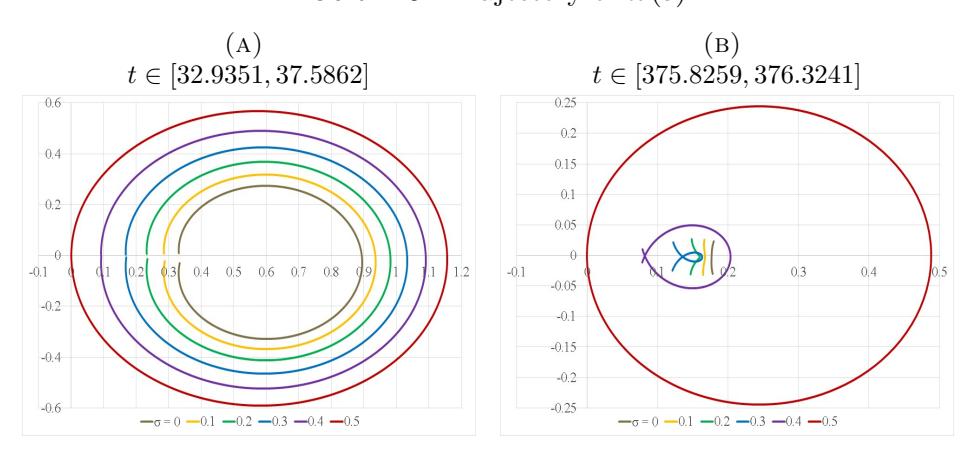


FIGURE 29. Trajectory of $\varpi(s)$.

Theorem 11. The Riemann hypothesis is true.

Proof. From lemma 24, it results that all the trajectories of the function $\varpi(s)$ are strictly within the area delimited by $\varpi(1/2+i.t)$, after t ordinate reaches the first zero of the Zeta function, therefore no intersection with

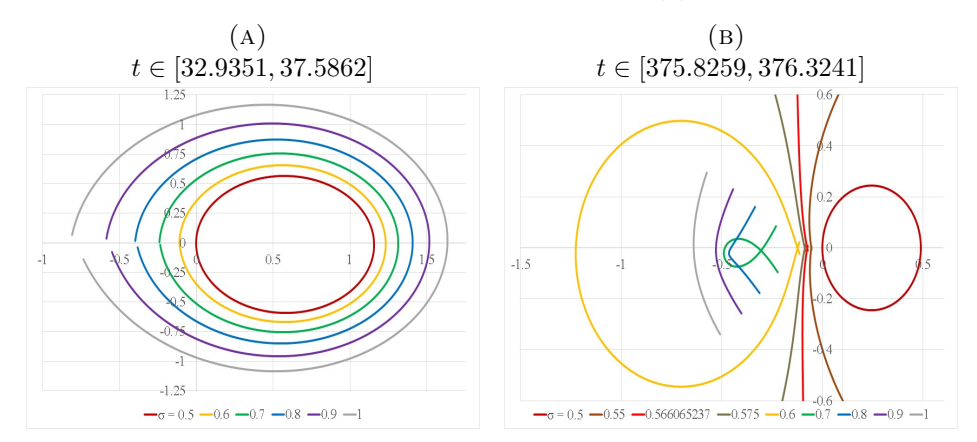


FIGURE 30. Trajectory of $\varpi(s)$.

the coordinate (0,0) is possible. Hence, no intersection with its numerator $\zeta(s)$ is neither practicable. This is so as long as $\zeta'(s) \neq 0$ as we emphasized in lemma 23. But, if not so, $\varpi(1/2+i.t)$ is diverging on the left and on the right side of $\sigma = 1/2$ designing some kind of approximative line when seen from some distance. We know that the multiplicative inverse of that kind of feature resembles a circle or at least a closed loop according to lemma 22, where in fact we started with a straight line 1/2 + i.t, hence a contradiction.

7. The partial cancellations' network

The sinusoidal feature, embedded in the Zeta function away from the critical band, allows the pairings of the partial and total cancellations sets. The existence of the pairings, by itself, is tempting for confirming the Riemann hypothesis as additional zeros outside the critical line would create necessarily havoc in these associations. In this section, we will take some distance from the critical line, to examine the network $Re(\zeta(s)) = 0$ (or $Im(\zeta(s)) = 0$) and its "well-behaviour" which any exception to the Riemann hypothesis would have certainly disturb a lot.

We will adopt in this section the convention $s = \alpha + i\beta$ in order to construct another reference where s is also expressed as a function of a and b and navigate between the two points of view.

The point here is to discover a regularity in the intersections of the Zeta function with the real axis which would likely not exist in the case of non-trivial zeros outside the critical line.

7.1. Covering the left half critical band. In order to examine the entire $0 < \alpha < 1/2$ domain, we consider the set of circles of radius 1/4 + a and centre (1/4 - a, 0), where $a \in]-1/4, \infty[$. All of these circles are tangent to point (1/2, 0) on the left side, and continuously increasing a, one will cover the entire targeted area (and more).

The parametrized equation of each of these circles, a being fixed, is then given in complex representation by:

$$1/4 - a + (a + 1/4).(\cos(2\pi t) + i.\sin(2\pi t))$$

where t describes a 1-length interval, for example:

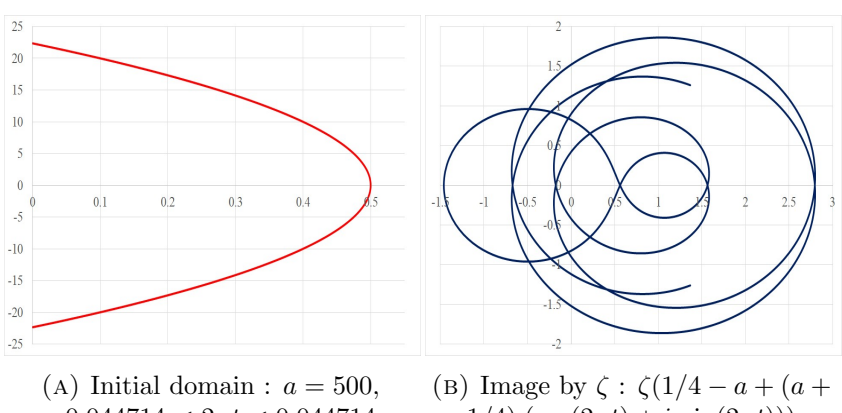
$$-1/2 < t \le 1/2$$

For t = 0, we get $1/4 - a + (a + 1/4) \cdot (\cos(2\pi t) + i \cdot \sin(2\pi t)) = 1/2 + 0 \cdot i$. For $t = \pm 1/2$, we get $1/4 - a + (a + 1/4) \cdot (\cos(2\pi t) + i \cdot \sin(2\pi t)) = -2a + 0 \cdot i$.

If we wish to reduce the points of the initial domain to $0 < \alpha < 1/2$, it suffices to restrict the previous domain of t to $0 < 1/4 - a + (a+1/4) \cdot \cos(2\pi t) < 1/4 - a + (a+1/4) \cdot \cos(2\pi t)$ 1/2, that is

$$-a\cos((a-1/4)/(a+1/4))/2\pi < t < 0$$

to which we may add the symmetric with respect to the α -axis. Doing so, we get for example the mapping from figure 31a to figure 31b (the left figure being a piece of a circle).



 $-0.044714 < 2\pi t < 0.044714$

1/4). $(\cos(2\pi t) + i.\sin(2\pi t))$

Figure 31

However, due to considerations appearing in the context of this article later on, it is quite more appropriate to take into account the whole domain $-1/2 < t \le 1/2$ (or $0 \le t \le 1/2$) rather than the above restriction.

Hence, the domains of definition are an infinite set of circles inscribed in each other. In figure 32, we provide a sample where parameter a takes integer values between 0 and 8, the intermediate circles not being represented. The left half critical band is situated on the right side of that figure.

One can then choose to navigate from one set of coordinates (a, t) to the other set (α, β) :

$$\alpha = 1/4 - a + (a + 1/4) \cdot \cos(2\pi t)$$

$$\beta = (a + 1/4) \cdot \sin(2\pi t)$$
(1)

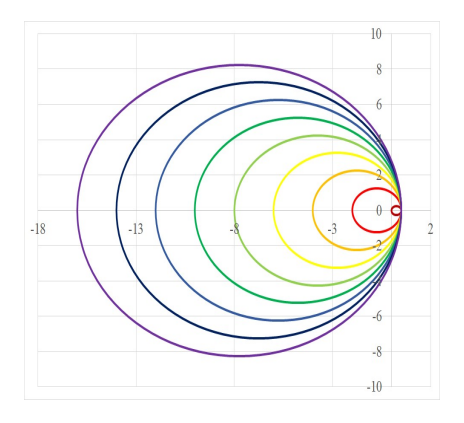


FIGURE 32. Domain of definition : a = 0 to a = 8, $a \in N$

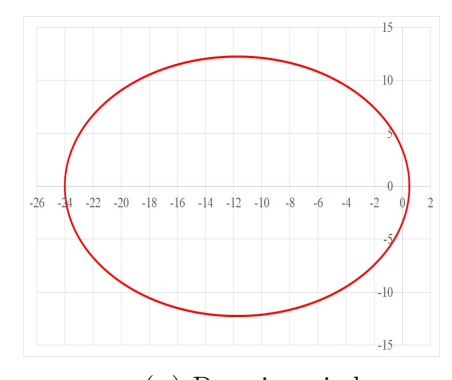
or from the set of coordinates (α, β) to the other set (a, t), using the value of parameter a found in the first expression for the second one underneath:

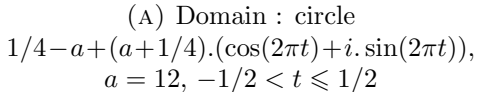
$$a = \frac{1}{2} \frac{(1/4 - \alpha)^2 + (\beta - 1/4)(\beta + 1/4)}{1/2 - \alpha}$$

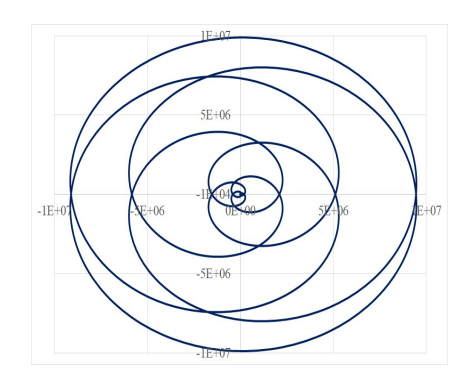
$$t = \frac{1}{2\pi} a sin(\frac{\beta}{a + 1/4}) = \frac{1}{2\pi} a sin(2(\frac{1}{2} - \alpha) \frac{\beta}{(1/2 - \alpha)^2 + \beta^2})$$
(2)

Note that if in this case $\alpha = 1/2$ then a is undefined and t = 0.

7.2. **Axis intersections.** A typical example of the domains and codomains of the previously mentioned circles, choosing a=12, gives the mapping from figure 33a to figure 33b.







(B) Codomain by ζ : $\zeta(1/4 - a + (a + 1/4).(\cos(2\pi t) + i.\sin(2\pi t)))$

Figure 33

The symmetry, in respect with the y = 0 axis, of the initial circle, due to the functional equation, implies the symmetry of the image versus the same

axis. Making the choice to take only positive values as an initial domain, the transformation from domain to codomain is as illustrated in figure 34a and figure 34b.

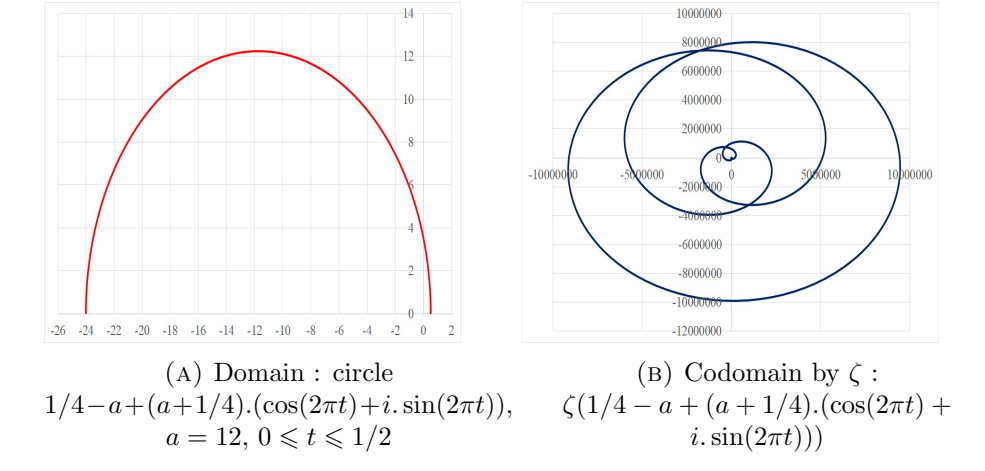


Figure 34

Let us consider then the codomain figures. We are going to collect some data on the set of intersections with the x = 0 and y = 0 axis.

Proposition 1. The number of intersections #I with the x-axis is equal to a over the domain $0 \le t < 1/2$, for any value of a equal to a strictly positive integer. For a = 0, the number of intersections is equal to 1.

The underneath additional note is a direct consequence of the previous proposition. We provide it in order to make easier the reading (and checking) of the various graphics using sometimes $-\pi < t \leqslant \pi$ and sometimes $0 \leqslant t < \pi$ as domains of definition.

Note. The number of intersections, distinct or not, $\#I_1$ with the x-axis is equal to 2a over the domain $-1/2 < t \le 1/2$ for any value of a equal to a strictly positive integer. The number of distinct intersections $\#I_2$ with the x-axis over the same domain is equal to a+1 for any value of a equal to a strictly positive integer.

$$\#I_1 = 2a, \ \#I_2 = a+1, \ a \in N^*$$

Besides for a = 0, we get

$$\#I_1 = 2 \text{ and } \#I_2 = 2$$

Proposition 2. The intersections with the y-axis are all distinct. The number of intersections #I with the y-axis is equal to a over the domain

 $0 \le t \le 1/2$ for any value of $a = n + \epsilon$, where $n \in N$ and $0 < \epsilon < 1$, N the natural numbers including 0.

$$\#I = n \setminus a = n + \epsilon, \ 0 < \epsilon < 1$$

Note. If $a \in N$, there are a few cases a < 3 to distinguish from the general result:

$$\begin{split} \#I &= 0 \quad if \quad a = 0 \\ \#I &= 2 \quad if \quad a = 1 \\ \#I &= 3 \quad if \quad a = 2 \\ \#I &= a \quad if \quad a \in N \cap a \geq 3 \end{split}$$

Note. The number of intersections (all distinct) $\#I_1$ with the y-axis is equal to 2n over the domain $-1/2 < t \le 1/2$ for any value of $a = n + \epsilon$, where $n \in N$ and $0 < \epsilon < 1$. The number of intersections $\#I_2$ with the y-axis over the same domain is equal to 2a - 1 for any value of a equal to a strictly positive integer except for a = 0 ($\#I_2 = 0$) and a = 1 ($\#I_2 = 3$).

$$\#I_1 = 2n$$
 if $a = n + \epsilon, \ 0 < \epsilon < 1$
 $\#I_2 = 0$ if $a = 0$
 $\#I_2 = 3$ if $a = 1$
 $\#I_2 = 2a - 1$ if $a \in N - \{0, 1\}$

Proposition 3. The value of the mantissa of a, for which an increase of the number of intersections #I with the x-axis occurs, is strictly increasing and bounded by 1 excluded when a tends towards infinity.

$$mantissa(a) = a - |a| \rightarrow 1^-, \ a \rightarrow +\infty, \#I \rightarrow \#I + 1$$

Proposition 4. The approximate interpolation of the value of the mantissa, linked to the intersections' cardinal #I increase, is given by:

$$mantissa(a) = 1 - 0.615(a + 0.5)^{-0.33}$$
 (3)

The corresponding data are given in table 3 and figure 35.

Note. To be precise, the depiction of the mantissa is not a continuous function as it takes actual values only when the number of intersections #I with the x-axis increases.

Note. The presence of a non-trivial zero would cause havor to a rule of thumb for the number of intersections and to the previous mantissa formula's smooth match.

Proposition 5. Similarly, but in a much simpler way as for the x-axis, the number of intersections #I with the y-axis increases with the value of a each time parameter a reaches an integer value, that is each time the mantissa of a cancels:

$$mantissa(a) = 0 (4)$$

$\mid n \mid$	a	mantissa	approx	n	a	mantissa	approx
1	1.358632	0.358632	0.353276	20	20.780205	0.780205	0.772207
2	2.468381	0.468381	0.508165	30	30.808699	0.808699	0.800493
3	3.537299	0.537299	0.573760	40	40.825408	0.825408	0.818434
4	4.585247	0.585247	0.613479	50	50.836720	0.836720	0.831246
5	5.620606	0.620606	0.641244	60	60.845044	0.845044	0.841050
6	6.647788	0.647788	0.662248	70	70.851511	0.851511	0.848896
7	7.669365	0.669365	0.678955	80	80.856731	0.856731	0.855384
8	8.686942	0.686942	0.692712	90	90.861066	0.861066	0.860876
9	9.701567	0.701567	0.704334	100	100.864746	0.864746	0.865614
10	10.713951	0.713951	0.714345	110	110.867923	0.867923	0.869762
15	15.755717	0.755717	0.749768	120	120.870705	0.870705	0.873438

Table 3. Mantissa values

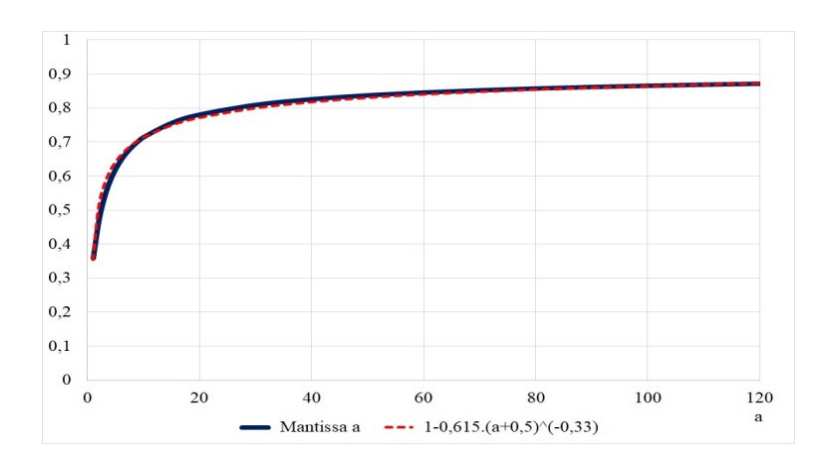


FIGURE 35. Mantissa of a matching an increase of the number of intersections #I.

Note. The triviality of the mantissa of a, guiding the increase of the number of intersections with the y-axis, is a mirror indicator of some expected "triviality" of the mantissa a relative to the x-axis, this latter triviality being the smooth evolution shown in figure 35. Therefore, we get again a reminder that non-trivial zeros outside s = 1/2 are not relevant.

In the rest of this article, we will focus on the x-axis intersections. Let us however note the existence of the same kind of pattern for the y-axis intersections.

Proposition 6. Let us have the explicit function of two variables $\zeta(a,t) = \zeta(1/4 - a + (a + 1/4).(\cos(2\pi t) + i.\sin(2\pi t)))$. We consider the implicit application t(a) such as $Im(\zeta(a,t)) = 0$. It defines a network of continuous values t of the variable a with an additional curve for each incrementation of #I, #I being the term defined in proposition 1.

a	1	2	3	4	5	6	7	8	9
S0	0	0	0	0	0	0	0	0	0
S1	π	0.4567π	0.3064π	0.2350π	0.1916π	0.1621π	0.1407π	0.1244π	0.1115π
S2		π	0.7124π	0.5769π	0.5117π	0.4749π	0.4545π	0.4454π	0.4449π
S3			π	0.8202π	0.7033π	0.6446π	0.6099π	0.5886π	0.5757π
S4				π	0.8766π	0.7751π	0.7208π	0.6865π	0.6637π
S5					π	0.9096π	0.8216π	0.7713π	0.7380π
S6						π	0.9306π	0.8538π	0.8074π
S7							π	0.9446π	0.8773π
S8								π	0.9545π
S9									π

Table 4. Sample of values $u = 2\pi t(a)$

Table 5. Sample of values $u = 2\pi t(a)$

a	6	6.2	6.4	6.6	6.647788	6.8	7
S0	0	0	0	0	0	0	0
S1	0.1621π	0.1573π	0.1528π	0.1485π	0.1476π	0.1445π	0.1407π
S2	0.4749π	0.4697π	0.4651π	0.4610π	0.4602π	0.4575π	0.4545π
S3	0.6446π	0.6363π	0.6287π	0.6218π	0.6203π	0.6156π	0.6099π
S4	0.7751π	0.7619π	0.7501π	0.7393π	0.7369π	0.7296π	0.7208π
S5	0.9096π	0.8864π	0.8669π	0.8499π	0.8461π	0.8349π	0.8216π
S6	π	π	π	π	π	0.9556π	0.9306π
S7					π	π	π

The data t(a), for a sample of integer values of a, are given in table 4. Each line corresponds to an additional curve.

Following the curves' trajectories imposed by keeping $Im(\zeta(1/4-a+(a+1/4).(\cos(2\pi t)+i.\sin(2\pi t))))=0$, we get the intermediary values of table 5 for a between 6 and 7, the reader will note the beginning of a new junction for the mantissa approximative value 6.647788 (as previously mentioned in table 3). The ordinate t=1/2 (written twice therefore) splits here into two values as the abscissa a increases.

The corresponding graphic representation is given by figure 36.

These are the curves which prolongation is linked to the trivial zeros of the Zeta function. One can observe a void between the first of the curve (excluding S0 the trivial t=0 line) and the other ones. The reason of this empty space is that it's not the full picture which one is given in figure 37. There, we have been completing it by the curves aiming at the non-trivial zeros and the partial zeros, something one could check with a careful tracking.

Note. The Zeta function is a smooth expression. With Occam's razor principle, it is difficult to imagine, in the initial $\sum \frac{1}{n^s}$, what would change the

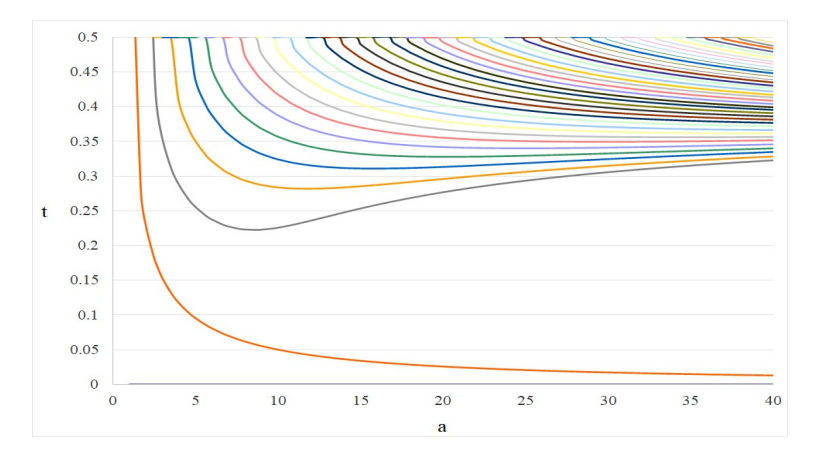


FIGURE 36. Network of curves t(a) such that $Im(\zeta(1/4-a+(a+1/4).(\cos(2\pi t)+i.\sin(2\pi t))))=0$

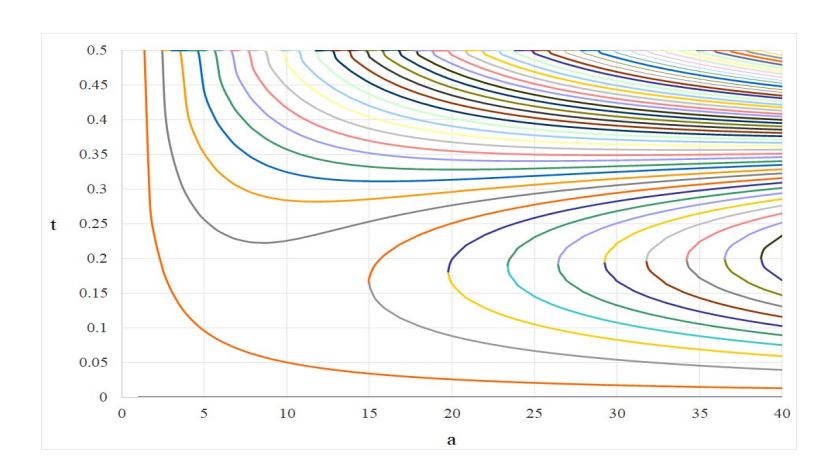


FIGURE 37. Network of curves t(a) such that $Im(\zeta(1/4 - a + (a + 1/4).(\cos(2\pi t) + i.\sin(2\pi t)))) = 0$

regular evolution of the network of curves shown in figure 37 on its way to infinity (a increasing). Of course, any non-trivial zero, outside Re(s) = 1/2, would create quite some havoc in this pattern.

Note. One can also represent the network of curves $Im(\zeta(1/4 - a + (a + 1/4).(\cos(2\pi t) + i.\sin(2\pi t)))) = 0$ within the system of coordinates (α, β) where α and β is defined by the equations labelled (1). The corresponding network is displayed in figure 38. This representation is however less appealing as the two patterns intermingle with confusing intersections while figure 37 allows to avoid that kind of phenomena. The diagonal pattern corresponds to the curves heading to the trivial zeros, the "partially horizontal" pattern heading towards the non-trivial zeros and their pairings in

an totally ordered manner. One can trace the link from one figure to the another by the corresponding colors of the curves.

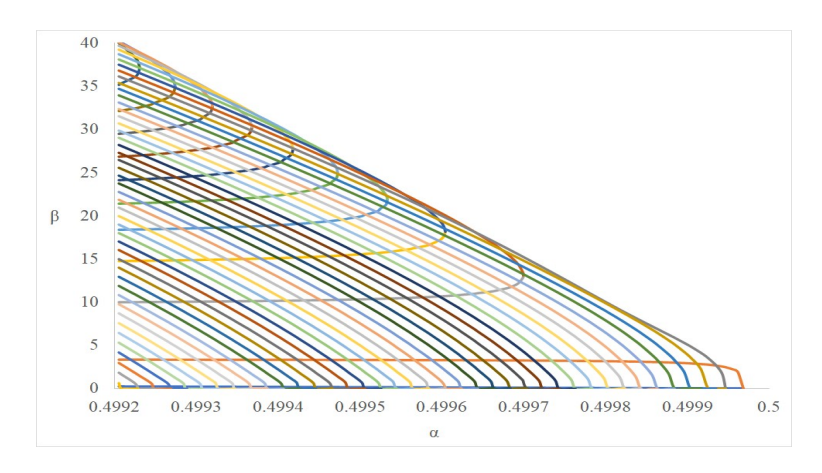


FIGURE 38. Network of curves (α, β) such that $Im(\zeta(1/4 - a + (a + 1/4).(\cos(2\pi t) + i.\sin(2\pi t)))) = 0$

LITERATURE AND SOURCES

- [1] Bernhard Riemann. Ueber die Anzahl der Primzahlen unter einer gegebenen Grosse. Monatsberichte der Berliner Akademie. Nov 1859.
- [2] Luis Báez-Duarte. Fast proof of functional equation for $\zeta(s)$. 14 May 2003 (arXiv math/0305191).
- [3] Tom M. Apóstol. Formulas for higher derivatives of the Riemann Zeta function Mathematics of computation. Vol 44, Num 169. Jan. 1985, p 223-232.
- [4] Andreas Speiser. Geometrisches zur Riemannschen Zetafunktion. Mathematische Annalen. Band 110, 6.4.1934, p 514-521.
- [5] Xavier Gourdon and Pascal Sebah.
 Numerical evaluation of the Riemann Zeta-function. July 23, 2003.
 //numbers.computation.free.fr/Constants/constants.html
- [6] Tristan Needham. Roger Penrose. Visual Complex Analysis. Oxford University Press, Feb 7, 2023.
- [7] 3Blue1Brown. Visualizing the Riemann Zeta function and analytic continuation. https://www.youtube.com/watch?v=sD0NjbwqlYw
- [8] Database of L-functions, modular forms, and related objects. https://www.lmfdb.org/zeros/Zeta/
- [9] Andrew M. Odlyzko home page https://www-users.cse.umn.edu/odlyzko/
- [10] https://en.wikipedia.org/wiki/Riemann_hypothesis
- [11] https://en.wikipedia.org/wiki/Riemann_Zeta_function
- [12] https://en.wikipedia.org/wiki/Digamma_function
- [13] https://en.wikipedia.org/wiki/Conformal_map
- [14] https://en.wikipedia.org/wiki/Zeros_and_poles https://fr.wikipedia.org/wiki/Zéro_d'une_fonction_holomorphe
- [15] https://en.wikipedia.org/wiki/Analytic_function
- [16] https://fr.wikipedia.org/wiki/Limite_(mathématiques) Limite et relation d'ordre.
- [17] https://fr.wikipedia.org/wiki/Limite_d'une_suite https://en.wikipedia.org/wiki/Convergent_series

INPG GRENOBLE

Email address: hubert.schaetzel@wanadoo.fr

 URL : https://hubertschaetzel.wixsite.com/website